BRNO UNIVERSITY OF TECHNOLOGY
VYSOKÉ UČENÍ TECHNICKÉ V BRNĚ

FACULTY OF ELECTRICAL ENGINEERING AND COMMUNICATION
FAKULTA ELEKTROTECHNIKY
A KOMUNIKAČNÍCH TECHNOLOGIÍ

DEPARTMENT OF FOREIGN LANGUAGES
ÚSTAV JAZYKŮ

THE JUNO MISSION TO JUPITER
MISE JUNO K JUPITERU

BACHELOR'S THESIS
BAKALÁŘSKÁ PRÁCE

AUTHOR
AUTOR PRÁCE
Jiří Gall

SUPERVISOR
VEDOUCÍ PRÁCE
M. A. Kenneth Froehling

BRNO 2020

VYSOKÉ UČENÍ TECHNICKÉ V BRNĚ
FAKULTA ELEKTROTECHNIKY A KOMUNIKAČNÍCH TECHNOLOGIÍ

Bakalářská práce

bakalářský studijní obor **Angličtina v elektrotechnice a informatice**

Ústav jazyků

Student: Jiří Gall ***ID:*** 203149
Ročník: 3 ***Akademický rok:*** 2019/20

NÁZEV TÉMATU:

Mise Juno k Jupiteru

POKYNY PRO VYPRACOVÁNÍ:

Cílem bakalářské práce je posoudit misi Juno k Jupiteru, skládající se vesmírné sondy NASA, která tuto planetu obíhá. Po stručné historii průzkumu vesmíru a předchozích misí k Jupiteru bude uvedeno poslání mise Juno a bude popsána kosmická sonda zaměřená na mikrovlnnou a elektromagnetickou technologii. Úspěchy poslání Juno budou komentovány a student se vyjádří k budoucnosti mise a kosmického průzkumu Jupitera.

DOPORUČENÁ LITERATURA:

Jupiter (Kosmos). Sheehan, William and Hockey, Thomas. Reaktion Books Ltd., London, 2018. 192 pp. ISBN10: 1780239084, ISBN13: 9781780239088

Bolton, S.J and Connerney, J.E.P. Editorial: Topical Collection of the Juno Mission Science Objectives, Instruments, and Implementation. https://link.springer.com/content/pdf/10.1007%2Fs11214-017-0430-0.pdf

Bolton, S.J. et al. The Juno Mission.

https://link.springer.com/content/pdf/10.1007%2Fs11214-017-0429-6.pdf

Connerney, J.E.P. et al. The Juno Magnetic Field Investigation.

https://link.springer.com/content/pdf/10.1007%2Fs11214-017-0334-z.pdf

Janssen, M.A. et al. MWR: Microwave Radiometer for the Juno Mission to Jupiter.

https://link.springer.com/content/pdf/10.1007%2Fs11214-017-0349-5.pdf

Termín zadání: 6.2.2020 ***Termín odevzdání:*** 12.6.2020

Vedoucí práce: M. A. Kenneth Froehling

doc. PhDr. Milena Krhutová, Ph.D.
předseda oborové rady

UPOZORNĚNÍ:
Autor bakalářské práce nesmí při vytváření bakalářské práce porušit autorská práva třetích osob, zejména nesmí zasahovat nedovoleným způsobem do cizích autorských práv osobnostních a musí si být plně vědom následků porušení ustanovení § 11 a následujících autorského zákona č. 121/2000 Sb., včetně možných trestněprávních důsledků vyplývajících z ustanovení části druhé, hlavy VI. díl 4 Trestního zákoníku č.40/2009 Sb.

Abstrakt

Semestrální práce je zaměřena na zkoumání planety Jupiter sondou Juno. Jsou zde popsány mise k Jupiteru, které předcházely misi Juno, spolu s jejich dosaženými výsledky. Dále je v této práci popsaná samotná mise Juno se zaměřením na zkoumání vzniku a následného vývoje planety. Je zde popsán průběh mise od startu až po, ještě neuskutečněné, shození sondy do atmosféry planety. Poté jsou popsány konstrukční prvky a subsystémy vesmírné sondy, spolu se všemi devíti měřícími přístroji určenými ke zkoumání planety. Na závěr jsou popsány a okomentovány její dosavadní výsledky.

Klíčová slova

Juno, Jupiter, Sluneční soustava, průzkum vesmíru, kosmická sonda

Abstract

The semestral thesis focuses on the exploration of the planet Jupiter by the Juno spacecraft. In this paper are outlined missions to Jupiter prior the Juno with the goals they achieved. Then the work focuses solely on the Juno mission, whose goal is to understand the origin and formation of Jupiter. Furthermore, is described mission timeline since launch to the mission deorbit. Following with the description of the spacecraft construction design and the various subsystem, along with the nine instruments implemented for the planet’s investigation. are described and comment preliminary results of the Juno mission.

Keywords

Juno, Jupiter, Solar system, space exploration, Jovian system, space probe

Rozšířený Abstrakt

Semestrální práce se zabývá misí Juno k Jupiteru z programu Nové hranice, který je veden NASA. Cílem této mise je určit vznik a následný vývoj planety Jupiter, což by přispělo nejen k porozumění planety samotné, ale také Sluneční soustavy v jejích prvopočátcích. Aby bylo možné tyto otázky zodpovědět, sonda zmapuje gravitační a magnetické pole planety, prozkoumá polární oblasti se zaměřením na solární záři a šíření vysoce energetických částic v polární magnetosféře, dále určí složení dynamické atmosféry a její vnitřní strukturu, poslední z cílů je podíl vody a amoniaku v atmosféře.

Pro zkoumání těchto 4 hlavních úkolů je sonda Juno vybavena 9 měřícími přístroji. Gravitační experiment GS měří, skrze Dopplerův jev, odchylku mezi telekomunikačním subsystémem sondy a sítí antén v zařízeních Deep Space Network. Magnetometr MAG mapuje magnetické pole k vytvoření jeho třírozměrného modelu, který dále pomůže s určením vnitřních struktur planety a jejich dynamiky. Mikrovlnný radiometr MWR pomocí svých 6 antén zkoumá různé oblasti atmosféry. Každá z antén má jinou frekvenci a délku vlny, čímž je umožněno zkoumání různých hloubek atmosféry. Ultrafialový spektrograf UVS zkoumá emise polárních oblastí v dalekém ultrafialovém (68–210 nm) a extrémním ultrafialovém (124–10 nm) rozsahu. Detektor energetických částic JEDI, zkoumá prostředí v polárních oblastech se zaměřením na magnetosféra a vznik polárních září. Dynamický polární experiment JADE měří ionty a elektrony s nízkou energií, které vytvářejí polární záři v magnetosféře planety. Infračervený mapovací spektrometr JIRAM pořizuje snímky v infračerveném spektru, s jejichž pomocí určuje složení atmosféry. Poslední z přístrojů je JunoCam, který pořizuje snímky planety, ale jeho účel slouží také veřejnosti.

V práci jsou také popsány konstrukční prvky a subsystémy sondy Juno. K ochraně před silně radiačním prostředí Jupiteru je sonda vybavena protiradiačním krytem, ve kterém se nachází citlivá elektronika. Sonda se skládá z několika subsystému, každý zajišťující jinou funkci. Výkonový subsystém řídí a distribuuje proud generovaný solárními panely, které jsou připevněné na všech 3 křídlech sondy o celkovém rozpětí 20 m. Tyto solární panely se skládají ze tří GaAs přechodů a jsou ošetřeny pro podmínky s nízkým zářením a teplotami (LILT). Generovaná elektrická energie je poté rozváděna po sondě pomocí jednotky pro Řízení a distribuci elektrické energie. Povelový systém a systém zpracování dat zahrnuje procesor RAD750, který pracuje na 200 MHz s 128 MB DRAM a 256 flash pamětí.

Subsystém pro řízení teploty pomáhá chladit Juno v blízkosti Slunce a zahřívat v joviánském systému, kde teplota dosahuje až -184° Celsia. Systém pohonu se skládá z hlavního raketového pohonu LEROS 1b, který je poháněn kombinací hydrazinového paliva a okysličovadlem ve formě oxidu dusičitého a zajišťuje zásadní změny kurzu. Pro menší změny kurzu a korekce trajektorie je použito 12 menších raketových pohonů, které využívají pouze hydrazinové palivo. Telekomunikační subsystém a DSN jsou součástí komunikačního systému, který zajišťuje komunikaci mezi zemí a sondou. DSN se skládá ze 3 zařízení umístěných ve Španělsku, v Austrálii a ve Spojených státech, které společně zajišťují nepřetržité spojení s Juno. Telekomunikační subsystém umožňuje přenos v UKV (X-band) a EKV (Ka-band) kmitočtovém pásmu. Běžná komunikace je zajištěna prostřednictvím UKV a EKV je součástí gravitačního experimentu.

Mise Juno byla zahájena 8. srpna 2011, kdy odstartoval nosná raketa Atlas V-551 se sondou Juno na palubě. Juno je sonda stabilizovaná rotací, proto byla krátce po startu roztočena na požadovanou hodnotu. K Jupiteru dorazila 5. července 2016, kdy podstoupila sestoupení na oběžnou dráhu Jupitera. Délka jednotlivých orbit byla změněna z původních 14denních na 53.5denní, z důvodu závady na hlavním pohonu. Jednotlivé orbity jsou od sebe odděleny 192° zeměpisné délky, což po 17. orbitách znamená kompletní pokrytí planety s 24° zeměpisné délky mezi jednotlivými orbitami. Po dosažení poslední 34. vědecké orbity je tato mezera zmenšena o dalších 12°. Po 34. orbitě je zahájenu sestoupení sondy do atmosféry Jupitera, kvůli ochraně Galileových měsíců Europy, Callisto a Ganymede.

Ke květnu roku 2020 bylo dokončeno 25 orbit z celkových 34. Sondě Juno se podařilo zmapovat gravitační pole planety. Tyto výsledky ukazují na hemisférickou asymetrii, která je pravděpodobně způsobena diferenciální rotací a hlubinnými atmosférickými proudy. Tato asymetrie spolu se symetrickou rotací planety utvářejí komplexní gravitační pole planety. Studie gravitačního pole také naznačuje možnou přítomnost kapalného jádra. Zkoumání magnetického pole přineslo vytvoření nového modelu tohoto pole s názvem JRM09, který ukazuje jeho sekulární variaci. Model také odhalil Velkou modrou skvrnu, která by mohla být zdrojem změn v magnetickém poli planety, a nedipolární magnetické pole v severní hemisféře. Měření v polární oblastech ukázalo, že by mohli být polární záře způsobeny částicemi, které se vynořují z atmosféry. Tyto částice jsou poté zrychleny plasmatickou vlnou a vyneseny do polární oblasti, kde poté působí na jiné částice různých energetický úrovní. Tato interakce vytváří polární záře, nicméně způsob, jakým jsou částice, které stojí za těmito zářemi, generovány není znám. Zkoumání atmosférických dynamik a vnitřní struktury

odhalily, že diferenciální rotace je potlačena v hloubce okolo 3000 km. Toto naznačuje rotaci pevného tělesa uvnitř planety. Dále Juno odhalila nejednotné rozložení amoniaku, který se ve velkém množství nachází v oblasti rovníků a také odhalila 0.25% koncentraci vody v atmosféře.

GALL, Jiří. Mise Juno k Jupiteru [online]. Brno, 2020 [cit. 2020-06-12]. Dostupné z: https://www.vutbr.cz/studenti/zav-prace/detail/127154. Bakalářská práce. Vysoké učení technické v Brně, Fakulta elektrotechniky a komunikačních technologií, Ústav jazyků. Vedoucí práce Kenneth Froehling.

Prohlášení

Prohlašuji, že semestrální práci na téma *Mise Juno do Jupiteru* jsem vypracoval samostatně pod vedením vedoucího semestrální práce a s použitím odborné literatury a dalších informačních zdrojů, které jsou všechny citovány v práci a uvedeny v seznamu literatury na konci práce.

Jako autor uvedené semestrální práce dále prohlašuji, že v souvislosti s vytvořením této práce jsem neporušil autorská práva třetích osob, zejména jsem nezasáhl nedovoleným způsobem do cizích autorských práv osobnostních a/nebo majetkových a jsem si plně vědom následků porušení ustanovení § 11 a následujících zákona č. 121/2000 Sb., o právu autorském, o právech souvisejících s právem autorským a o změně některých zákonů (autorský zákon), ve znění pozdějších předpisů, včetně možných trestněprávních důsledků vyplývajících z ustanovení části druhé, hlavy VI. díl 4 Trestního zákoníku č. 40/2009 Sb.

V Brně dne ....

Jiří Gall

Acknowledgement

I would like to express my gratitude to my supervisor, M.A. Kenneth Froehling, for his patience and guidance, which helped me complete the thesis in these uncertain times.

I would also like to thank my colleague, Karolína Čechová, for always finding some time to help me with my tasks.

Contents

INTRODUCTION

Juno is the second NASA mission of the “New Frontiers” program designed to study Jupiter. Juno is an unmanned spacecraft developed in cooperation with six institutions as PI-led mission and launched on August 5, 2011 with arrival in Jupiter orbit on July 4, 2016. There spacecraft investigates planet by following near-polar orbits until July 2021 with a three-years extension in 2018.

Jupiter’s enormous mass allowed perseverance of its original composition, hence the acquired data from planet’s investigation may further the understanding of its formation and evolution. Subsequently providing information correlating with formation of Solar System as Jupiter is the oldest planet within.

To meet the mission’s objectives Juno spacecraft is equipped with various microwave and electromagnetic instruments, specially designed to survive in harsh Jovian environment with the most vital electronics protected from radiation by a titanium vault. Additionally, the Juno mission is provided with cutting-edge solar cell technology for the spacecraft is planned to be the most distant solar-energy powered emissary.

The aim of this paper is to provide information on the missions to Jovian system prior to the mission Juno. State the goals and objectives of the mission and comment on the goals hitherto achieved. Describe the function and purpose of the spacecraft’s scientific instruments and various subsystems.

Name of the spacecraft Juno is derived from Roman mythology. Jupiter, the god of sky, possessed the ability of hiding behind the clouds, and only Juno was capabla to see through the shroud. Analogues to Juno mission, spacecraft peers through the Jupiter’s dense clouds and reveals the planets true nature to us (Juno Overview).

1. HISTORY OF EXPLORATION OF JUPITER

To understand the Juno mission, one must look at the findings of the previous spacecrafts that were either deliberately sent to Jupiter or passed the planet as part of their main mission.

1.1 Pioneer 10, 11

Pioneer 10 was launched on March 2, 1972, and after 20 months on November 6, 1973, reached Jupiter with goals to flyby Jupiter and then on that trajectory leave the Solar System (Siddiqi, 1985). During the flyby of Jupiter, the probe took first close-up images of the gas giant and measured Jupiter's interior, atmosphere, magnetosphere, magnetic field, and radiation belts. The probe left the surroundings of Jupiter on January 2, 1974. Its discovery of Jupiter's strong radiation environment was essential in designing future spacecraft that should encounter Jupiter such as Voyager, Galileo, and Juno.

Pioneer 11 is the successor of Pioneer 10, launched on April 6, 1973, with intentions to study Jupiter and Saturn (Siddiqi, 1985). On its flyby of Jupiter took better images of the famous Great Red Spot, observed the planets polar regions change in magnetosphere as solar winds buffet it, and determined the mass of Callisto, the Jupiter's moon.

1.2 Voyager 1, 2

First, two Voyager spacecrafts were launch in 1977 and arrived at the Jovian system in 1979 and together they took more than 33,000 pictures of Jupiter and its moons.

Images of Voyager 1 showed material ejected into space as a result of significant volcanic activity on the moon Io. Furthermore, findings of a volcanic activity on Io

indicates an origin of sulfur and oxygen in the Jovian system. In addition to the Io findings, Voyager 1 took detailed pictures of surfaces of Europa, Ganymede, Callisto, Amalthea and also discovered two new moons: Metis and Thebe. Considering Jupiter, Voyager 1 had observed a more bustling atmosphere than Pioneer 10 and 11, which provided new data for redesigning the current atmospheric model of the planet (Siddiqi, 1985).

Voyager 2 flew closer to the Jovian system, which allowed the spacecraft to take closer images of Jovian moons: Amalthea, Callisto, Europa, Ganymede, Io; and discovered new moon: Adrastea. With the addition to Voyager 1 images, Scientists were able to map up to 80% of Callisto and Ganymede surfaces. Pictures of Europe surface display crossed lines that indicate ice cracks (Siddiqi, 1985).

1.3 Galileo

Galileo mission consisted of an orbiter and an atmospheric probe, which were both delivered to Earth orbit by Space Shuttle Atlantis on October 18, 1989. The spacecraft followed VEEGA (Venus-Earth-Earth Gravity Assist) trajectory to gain enough velocity from a gravitational slingshot for the voyage to Jupiter where it arrived on December 7, 1995. The probe was released 145 days prior to the arrival of the Orbiter to Jupiter with purpose to examine its atmosphere. The probe descended into Jupiter's atmosphere and operated for an hour before being destroyed by the rough conditions on the planet. Obtained data from the probe were then sent back to Earth via the orbiter that had already proceeded to enter the planet's orbit to start its 8-years-long observation of Jupiter (Siddiqi, 1985).

Important discoveries from the observation of Jupiter were the following:

- Magnetic field on the moon Ganymede - which makes it the first satellite to posses one
- Liquid water under the surface of Europa
- Potential subsurface ocean on the moon Callisto

- Io's lava - is composed of silicate material rich in magnesium since it is hotter than the lava on Earth
- Origin of Jupiter rings - they are composed of dust, which is ejected from the Jupiter's four innermost moons (Amalthea, Thebe, Metis and Adrastea)
- Helium composition of Jupiter - similar to the Sun's
- Jupiter´s giant thunderstorm – thousand times greater than on Earth
- Radiation belts above the cloud tops of Jupiter
- Water abundance – revealing a lesser amount of water components compared to The Sun
- Galileo's presence in the radiation environment – it helped to enhance the spacecraft´s hardware resistance due to higher radiation of the Jovian system

1.4 New Horizons

The New Horizons spacecraft was launched on January 19, 2006. It approached Jupiter on February 28, 2007, for a gravity assist maneuvre that consequently increased its velocity and shortened the amount of time needed to reach Pluto. During the four-month-long flyby period, the spacecraft tested its scientific payload on Jupiter and its moons Io and Callisto in particular.

New Horizon studied eleven volcanic eruptions on the moon Io, where three of them were observed for the first time. It detected some changes in the planet's atmosphere along with flashes of lightning in the polar regions. Spacecraft had been equipped with an advanced camera technology compared to the Galileo spacecraft. This advantage had been utilized, and the spacecraft took breathtakingly detailed images of Jupiter, Little red spot, Calisto, Io, and Europa (Siddiqi, 1985).

Closest approach of the New Horizons was at a distance 2,300,000 km for comparison Juno gets on its elliptical orbit up to 4,200 kilometres from the Jupiter's top cloud layer. This long-distance flyby of New Horizons spacecraft ensured the safety of

the scientific payload. Due to this fact, the spacecraft could not have executed a more precise observation of Jupiter's system.

2. MISSION OVERVIEW

2.1 Science Objectives of the Juno Mission

Exploration of Jupiter prior to the Juno mission shows composition primarily of hydrogen 90 % and helium 10 % in upper layers of the atmosphere (Coulter, 2011) significantly correlating with the Sun's composition. This indicates an early formation of the planet. Before the place of the Juno spacecraft in Jupiter's orbit, prevailing models of Jupiter origin are a core accretion model and a formation due to gravitational instability of protoplanetary disk.

In the core accretion model Jupiter experienced two-phased formation, firstly developing a rocky core and latter a gases envelope. However, such process requires more time than is a life cycle of protoplanetary disk (Shige,2001). The disk instability model, on the other hand, enables formation of Jupiter-size protoplanets within this cycle. In addition to the planet's formation models, Juno investigation implies how the Solar System evolved in its early stages. Thus, proving or disproving existing theories and concepts such as Nice model, Grand Tack hypothesis, and Hot Jupiter or creating new ones.

Juno mission consists of 4 primary scientific objectives (Bolton, Connerney, 2017):

1) Planet's gravity and magnetic field mapping
2) Investigation of polar regions, specifically generation of auroral zones and correlating magnetosphere and its distribution
3) Determination of atmospheric dynamics and its interior composition
4) Measurement of water and ammonia abundance

Measurement of those objectives may lead to determination of what type of core Jupiter possesses, thus uncovering history of the Jupiter's formation and evolution, as well as of the Solar System.

2.2 Mission Phases

Juno mission is conducted over a span of 10 years and separated into 5 phases. It started with thoroughly determined Launch phase to ensure the correct course of the subsequent Cruise phase. The Cruise phase begins shortly after the Launch phase and lasts rougly five years and cover a period between the launch and the arrival at Jupiter, the fifthe planet of the Solar System. At Jupiter, Juno goes through the Jupiter Orbit Insertion (JOI), which inserts the spacecraft into Jupiter orbit and the Period Reduction Maneuvers (PRM), which corrects the orbit length to intended nominal 14-days orbits. Once the 14-days orbit is established, an Orbital phase begins. During this phase, Juno performs a total of 33 science orbits to execute its primary scientific objectives. After Juno completes its scientific goals it is designed to fall into Jupiter during the Deorbit phase. Entire mission flight path is represented in the Figure 1.

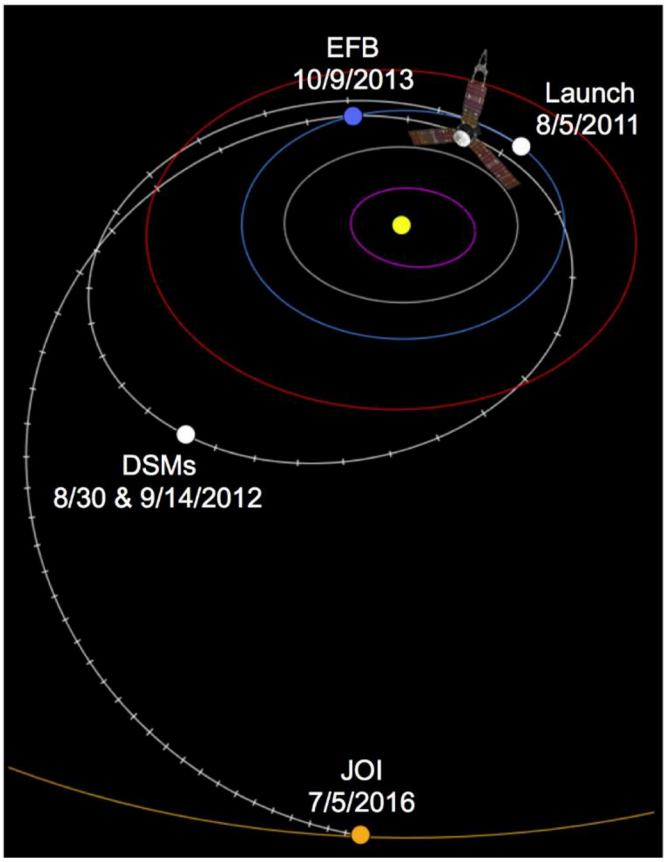

Figure 1 The Juno mission flight trajectory. EFB stand for the Earth Flyby.

2.2.1 Launch Phase

For the spacecraft to follow a predetermined trajectory, it had to be launched within 21-days launch window. Eventually, the launch took place on the very first day of the time window on August 5, 2011, at 16:25:00 of Universal Time on board of Atlas V-551 vehicle. Atlas delivered spacecraft to a parking orbit, where it coasted for 30 minutes to meet thermal limits and then proceeded to a heliocentric orbit. After stabilizion of the vehicle in the heliocentric orbit a payload fairing engineered to protect payloads during flies through the atmosphere is dropped. At this moment is initiated spin-up to 1 RPM (Juno Mission & Trajectory Design). Spinning allows better control and more stable pointing of the spacecraft, hence provide more precise measurement of the Jovian System. It also provides 360 field of view span as the spacecraft rotates about 250 times during its 2 hours Jupiter flyby (Press kit: Juno spacecraft). Additionally to post-separation sequence, Juno deployed its solar arrays to recharge the batteries, which–once recharged–provides electricity for a test of the scientific equipment. Launch phase is finished with transmission of launch telemetry data and acknowledgement of spacecraft's stability, health, and readiness to accept commands (Mukai, Ryan, 2017).

2.2.2 Cruise Phase

After the successeful Launch Phase Juno is set on a voyage to Jupiter, this nearly five years long period is called the Cruise Phase and is divided into several sub-phases. To achieve sufficient velocity to escape Sun's gravity and reach Jupiter a Venus-Earth gravity assist (2+ΔV-EGA) is employed roughly 2 years after launch.

Inner cruise 1 involves reporting on spacecraft' scientific instruments, tested before the Cruise Phase and checking spacecraft's telemetry data. 12 monopropellant thrusters are utilized to correct trajectory by some means altered by the Atlas V-551 vehicle. Whereas Inner cruise 1 took 63 days to complete, following Inner cruise 2 stretches over 597 days and includes two Deep Space Maneuvers (DSM). DSMs are essential part of the 2+ΔV-EGA. For better control, Juno is spinned to 5 RPM and by two

consequent fires of the main engine on August 30 and September 14, 2012, Juno is led to Earth for a gravitational slingshot. This provides the spacecraft with enough velocity to escape tremendous gravity of the Sun and reach Jupiter (Juno Mission & Trajectory Design). Furthermore, the maneuvers increase the spacecraft's speed up to approximately 265,00 km/h, making Juno the fastes human-made object in history. Previous record was held by Helios 2 with 253,000 km/h (Wall, 2016).

On May 27, 2013 Juno approaches a Mars orbit, hence entering the Inner Cruise 3. On October 10, in the same year, executes the Earth Flyby (EFB) for the necessary velocity gain and the additional testing and calibration of Juno payload. On November 4, 2013 the spacecraft enters another sub-phase called a Quiet Cruise, which lasts 791 days and covers an undisturbed path after the successful EFB all the way to Jupiter. Last of the Cruise sub-phases is called Jupiter Approach Phase and consists of 3 Trajectory Correction Maneuvers (TCM), which prepares Juno for the JOI.

Throughout the Cruise Phase, the spacecraft experiences significant changes in the distance with Earth. To maintain the connection, Juno utilizes all of its antennas. This is described in more deatil in the Antennas chapter.

2.2.3 Jupiter Orbit Insertion (JOI) and Period Reduction Maneuver (PRM) Phase

Since the JOI occurs at far distance, it cannot be performed in real time but needs to be automated. For this reason, necessary commands must be send beforehand the maneuver. Moreover, spacecraft must be spinned from 1RPM to 5 RPM. The orbit insertion was executed on July 5, 2016, 4 days after entering the JOI phase (the JOI is represented by perijove 0 in the Figure 3). The spacecraft fired its main engine for 35 minutes and navigated itself via the predetermined commands into a 107-days long Capture orbit of Jupiter, which is designed to avoid the harshest regions of the planets radiation belts as indicates Figure 2 (Juno Mission & Trajectory Design).

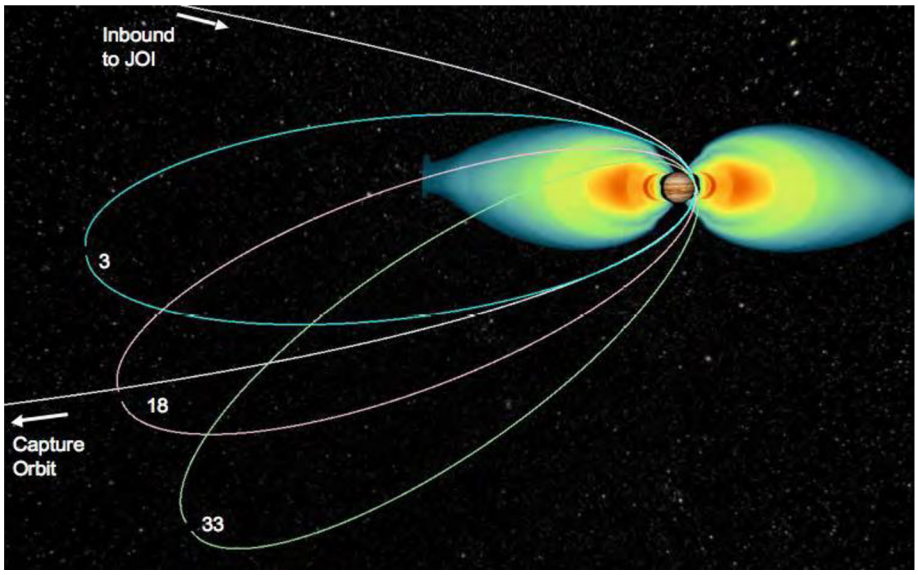

Figure 2 JOI with following Capture orbit and orbits 3,18, and 33 after PRM in comparison with the radiation belts of Jupiter

Due to need of the 33 science orbits, the initial 107-days long Capture orbit needs to be reduced to 14-days orbits, hence the Period Reduction Maneuver, which significantly lowers the time span of the mission. After the completion of the Capture orbits (represented by perijove 1 and 2 in the Figure 3) Juno fired its main engine again to lead the spacecraft to 14-days orbits. However, on October 19, 2016, Juno entered a safe mode, which was result of a problem in the main engine valves. Due to this complication, the spacecraft docked in 53.5-days long orbit, which are represented by orbits 3, 18 and 33 in the Figure **2**. As the spacecraft receive most of the radiation during perijoves (close fly-bys of the planet), the mission is not endangered by the orbit length extension.

2.2.4 Orbital Phase

Prior to the first scientific orbit, a perijove 3, on December 11, 2016, Juno is spinned up to the 2 RPM. Such rotation speed allows utilization of the instruments arranged around the spacecraft's body. The spacecraft follows a higly-elliptical polar orbit, a Figure 2 illustrates a high eccentricity of the orbit, while Figure 3**Chyba! Nenalezen zdroj odkazů.** shows a passage above both poles. The orbit trajectory brings

the spacecraft up to 4.200 km from cloud tops of the planet. Moreover, the orbits are designed to provide complete coverage of the planet, therefore each subsequent orbit is shifted by 192° resulting in 24° spacing between the perijoves by the 17th perijove. For the perijoves 18 to 34 the spacecraft employs a 180° orbit separation, thus providing even more detail coverage with 12° spacing after reaching a 34th perijove (Perijoves are depicted in the Figure 3). It is crucial for the the perijoves to be executed precisely, therefore after each perijove Juno undergo an Orbit Trim Maneuver (OTM) to make adjustments to its path (Kowalkowski, Johannesen, 2008).

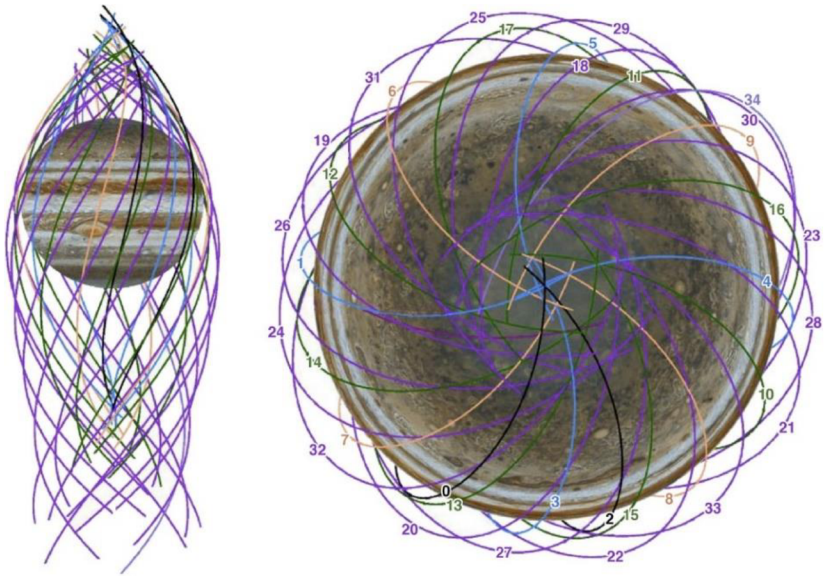

Figure 3 Individual perijoves and their even distribution around the planet with equator view on the left and north pole view on the right

2.2.5 Deorbit Phase

The Deorbit phase is planned after the final 34th perijove around July 2021. Juno will be purposefully put into Jupiter's atmosphere and destroyed. In case of keeping Juno in the orbit, there may be chance of collision with one of the Galilean moons. The moons Calisto, Ganymede, and Europa may potentially harbor an extraterrestial life, and possible collision with Juno may contaminate them with Earth life. This would be against the strict policies of the NASA's Planetary protection (Planetary Protection), hence the planned drop of the spacecraft into the planet's atmosphere (In Depth: Juno).

3. SPACECRAFT DESCRIPTION

The Juno spacecraft weights 3.625 kg along with wings span of 20 meters. To maintain such large system, spacecraft is divided into subsystem, each constructed to executed series of tasks they are specifically designed to. Together it ensures the spacecraft functions reliably during its mission.

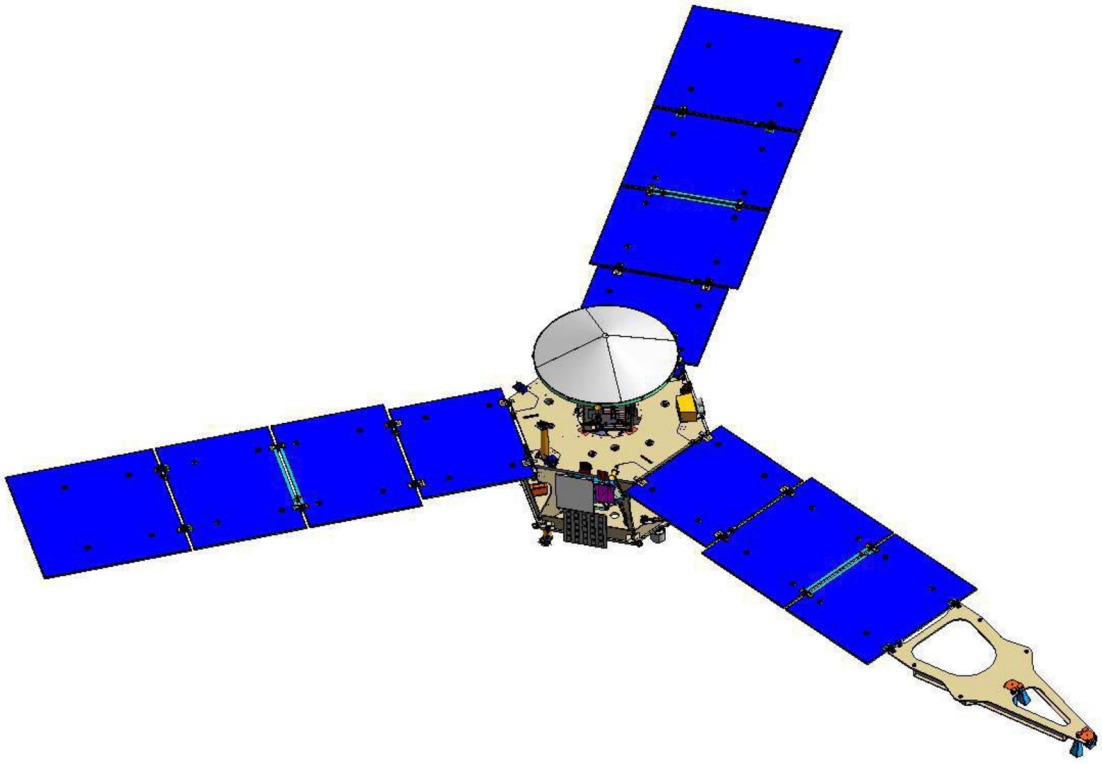

Figure 4 Front view on the Juno spacecraft

3.1 Radiation Vault

Jupiter along with its moons is protected from the solar wind, a stream of charged particles, by Jupiter's magnetic field. The solar wind is captured in the magnetic field and forms so-called Van Allen radiation belts and creating an intense radiation environment of Jupiter. Jupiter possesses magnetospheric ionizing radiation~20,000 times greater that

of Earth, which extends beyond the moon Europa at total distance of 650,000 km (Greicius, 2010).

To protect the Juno's vital electronics (e.g. Power and Data Distribution Unit, Command and Data Handling Box, and Electronics boxes of spacecraft's instruments.) was assembled the titanium vault. One-centimetre thick walls with an area size of one meter with a total weight of 200 kg ensure that the electronics of the Juno spacecraft can survive contact with the radiation environment of the Jovian system (Greicius, 2010).

3.2 Power Subsystem

3.2.1 Power Generation

The previous NASA deep-space probes such as Pioneers, Voyagers, and Galileo were powered by a nuclear radioisotope thermoelectric generator (RTG). In contrast Juno spacecraft is powered solely by solar energy resulting in a farthest solar-powered space exploration mission, when orbiting Jupiter. This is due to the technological progress in solar-cell technology over the years, allowing for generation of sufficient amount of electricity at the Jovian environment, which possesses 25 times less solar radiation than Earth. Also, a plutonium-fueled power source is much more demanding to produce than solar cells (Juno Spacecraft: Solar Arrays). Moreover, at the time of development of the Juno mission the space exploration industry was suffering a shortage of Plutonium-238, a fuel for RTGs (Dickinson, 2013). "*We decided it was probably less risky to advance technology of solar cell to work at Jupiter than it was to invent a new nuclear power source."* (Scott Bolton, Juno Spacecraft: Solar Arrays).

The electrical energy for the spacecraft to operate is produced by three evenly arranged solar arrays attached to the spacecraft main body. The arrays are divided into smaller solar panels, which guarantees their foldability for the launch phase of the mission. One panel at the end of the array is replaced with magnetometer boom affix, showed in the Figure 8. Therefore the solar arrays are composed of 11 panels in total. The

solar arrays are 2.7 meters wide and after deployment reach a length of 9 meters. Such size is necessary because Jovian system receives only 4 % of Earth's solar radiation. Furthermore, the solar cell technology must also operate in temperatures of -184° Celsius. For this low irradiance low temperature (LILT) conditions was selected GaAs ultra triple junction (UTJ) cell technology, which is also used for GEO and LEO satellites. Moreover, the cells were screened to avoid undesirable degradation of cells under the LILT conditions and shielded with coverglass against the ultraviolet radiation and charged particles (Dawson, Stella).

For comparion, the solar array wings are at the time of deployment capable of producing 12 kW, however at Jupiter, the arrays only produce about 400 W. Even though this is a significant drop, the Juno scientific payload runs only for about 6 hours during the perijoves and is designed to be highly energy saving. Thus, Juno can operate accordingly even that far in space (Juno Spacecraft: Solar Arrays).

3.2.2 Power Management and Distribution

The power generated by solar wing arrays is managed and distributed by the spacecraft's Electrical Power Subsystem consisting of a Power bus, Power Distribution and Drive Unit (PDDU), and two 55 amp-hour lithium-ion batteries.

To provide appropriate power generation for the spacecraft Juno switches between 3 types of strings depanding on the distance from the sun: long strings ranges from 0.85 to 1.9 AU, medium from 1.8 to 3.75 AU, short from 3.75 to 5.5 AU (Dawson, Stella). Power bus distributes required voltage levels to the instruments, heaters, propulsion. The PDDU manages and monitors Power bus to ensure proper power distribution and also manages the string switching. Albeit, Juno mission is designed to be in the maximum exposure to the Sun, batteries are necessesary in close-flybys of the planet, when is off-Sun or during ecplises. Batteries' state of charge is managed by the PDDU. (Kurth, 2012)

3.3 Command and Data Handling Subsystem (C&DH)

The C&DH is executed on the single-board and radiation-hardened RAD750 processor, which operates at up to 200 megahertz with 128 megabytes of DRAM local memory and 256 megabytes of flash memory. The processor meets the intruments throughput requirements of 100 Mbps and offers 17 Gbits of data storage. C&DH is a single tolerant system, meaning it endures only one incident requiring outside intervention in its lifespan. Albeit RAD750 is designed to withstand radiation environment, to cope with the Jovian it is located in the radiation vault (Press kit: Juno spacecraft).

3.4 Thermal Control Subsystem (TCS)

With the Thermal Control Subsystem, the Juno spacecraft is operationable at distant and cold Jovian system (5.2 AU) and in relatively close approaches to the Sun (1 AU). While close Sun encounters, the spacecraft is pointed in a manner, which allows a High Gain Antenna (HGA) to shade and protect both vaulted and outside electronics from overheating. However, at Jupiter the spacecraft is exposed to temperatures about -184° Celsius. To overcome such issue, Juno is equipped with the thermal control elements such as heaters and louvers. The heaters provide heat for the external instruments–each requiring a specific temperature limit–and to the vault electronics. The louvers on the other hand, manages excess heat through dissipation (Press kit: Juno spacecraft).

3.5 Propulsion Subsystem

Juno is equipped with the dual-mode Propulsion Subsystem allowing decrease of total weight of the spacecraft and redundancy. LEROS 1b, the main engine, is hypergolic bipropellant combining hydrazine fuel and nitrogen tetroxide oxidizer–stored separately in six propellant tanks–for thrust. The main engine is mounted on the spacecraft aft and utilized during major mission maneuvers such as JOI or DSMs. The latter part of the

propulsion subsystem utilizes 12 monopropellant Reaction Control System (RCS) thrusters installed aboard the spacecraft. For a thrust is burnt hydrazine without any oxidizer, hence monopropellant (Press kit: Juno spacecraft). Whereas the main engine allows significant alteration in trajectory, the lesser thrusters enables small trajectory, rotation, and orientation adjustment, for example TCM and OTM (Kurth, 2012).

4. COMMUCATION SYSTEM

The Communication System of Juno mission consists of space segment the Telecommunication subsystem of the Juno spacecraft and ground segment the Deep Space Network (DSN). The communication between the segments is devised to function with a significant delay caused by the great distance between Earth and Jupiter (approximately 5.2 AU). Therefore, Juno spacecraft executes task independently based on a list of commands from Earth, while reporting its status and gathered data (Juno Spacecraft: Communication system).

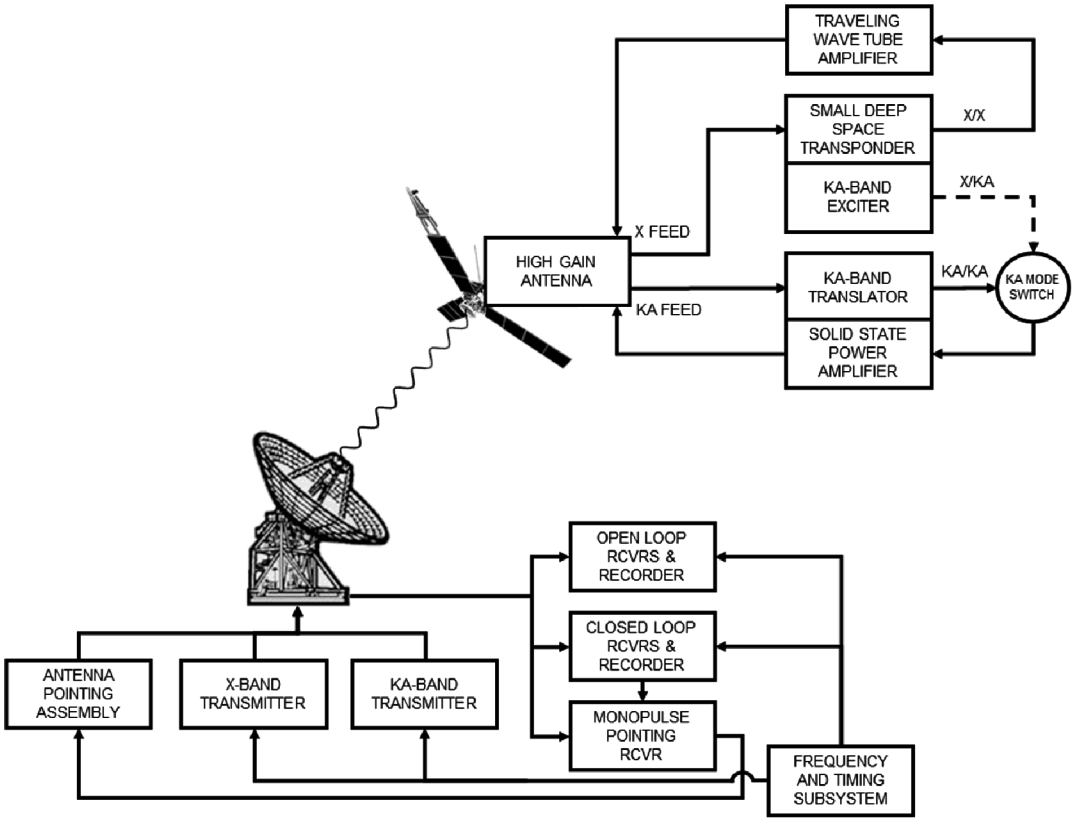

Figure 5 Communication system composed of the space segment (Telecommunication subsystrm) and ground segment (Deep Space Network).

4.1 The Deep Space Network (DSN)

"DSN is an international network of antennas that supports interplanetary spacecraft missions and radio and radar astronomy observations for the exploration of the solar system and the universe" (Deep Space Network). The facilities are arranged around

the world in Madrid, Spain; Goldstone, USA; and Canberra, Australia. To provide a full field of view coverage for continuous communication regardless of the Earth's rotation, stations are separated by approximately 120 degrees in the longitude.

Although each facility incorporates several antennas of various types, the Juno mission utilizes only 34-meter beam waveguide (BWG) and 70-meter antennas. During the JOI Juno experiences significant decrease in signal strength. To compensate this, facilities in Madrid and Goldstone employs all of their 9 antennas to guarantee reliable communication link. Nominal communication is executed over BWGs regardless of the facility. Because only one DSN facility is capable of Ka-band transmission, the Ka-band communication may take place only at one station in Goldstone, the DSS-25 in particular. At critical events and in case of the system falling into the safe mode spacecraft utilizes Madrid's DSS-63, which incorporates 70-meter antenna (Mukai, Ryan, 2017).

4.2 Telecommunication Subsystem

The spacecraft operates at the X-band with the exception of Gravity Science investigation, which provides dual-band support for two frequencies (X-band and Ka-band) to increase measurement accuracy. The X-band is used for a two-way communication (between the spacecraft and the DSN) with command (CMD) uplink of 7.153 GHz receiving frequency and telemetry (TLM) downlink of 8.404 GHz transmitting frequency. Another function utilized over the X-band is Radiometric Tracking. Juno possesses 3 systems for such function: Doppler tracking, which measures a shift in the frequency between the received and transmitted signal; two-way range tracking for determination of the spacecraft range through round-trip delay time (RTD) of a DSN generated signal; andan one-way Delta Differential One-way Ranging (ΔDOR), which determines the spacecraft's angular location.
In order to provide accurate data for the Radiometric tracking, a signal from two DSNs is necessary (Mukai, Ryan, 2017).

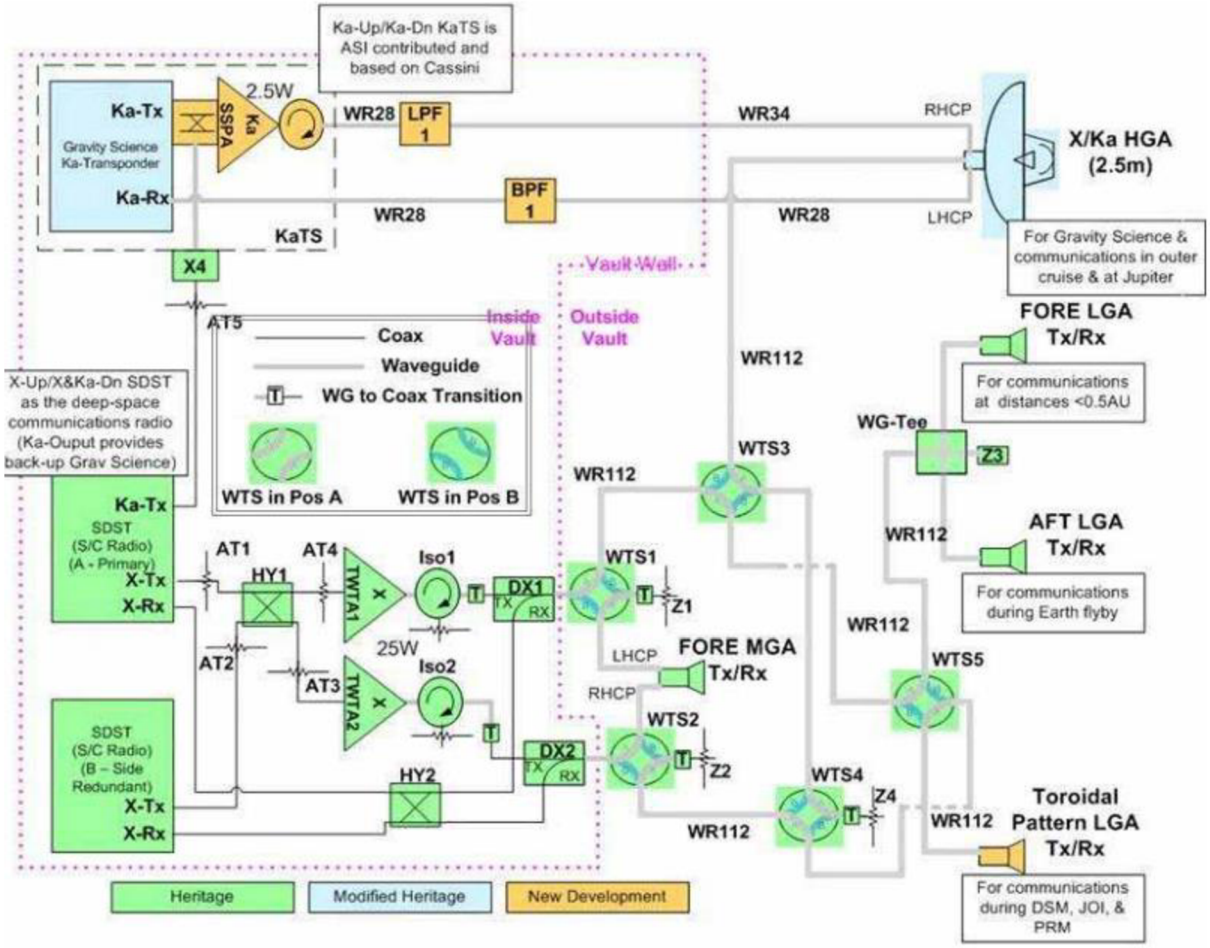

Figure 6 Schematic of the Telecom Subsystem of the Juno spacecraft

4.2.1 Antennas

Telecom subsystem consists of 5 antennas arranged on the fore and aft of the spacecraft aligned with Z-axis, with exception of the TLGA, which is angled by 90 degrees to provide full spherical coverage crucial during the DSM and JOI, when the spacecraft not directly points to Earth.

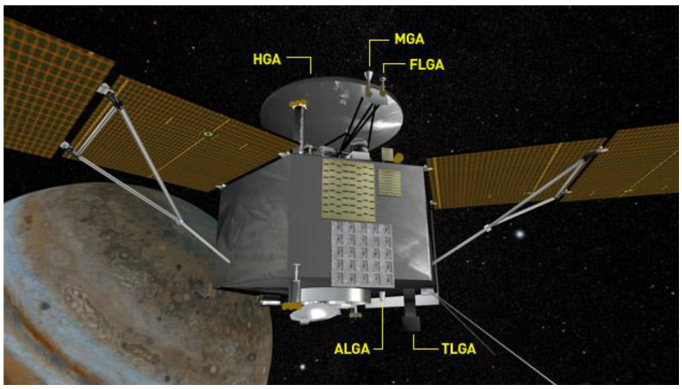

Figure 7 Juno's antenna arrangement

The antennas operate at X-bands with 7.1 GHz uplink and 8.4 GHz downlink and in case of HGA also at Ka-band with 34.4 GHz uplink and 32.1 GHz downlink

4.2.1.1 High Gain Antenna (HGA)

The HGA utilizes a parabolic antenna consisting of a dual-band corrugated feed antenna, a subreflector of Gregorian design, and parabolic reflector with 2.5 m in diameter conditioned by the operational wavelength of Ka-band (for the purpose of the GS investigation) and the X-band. The antenna's components have a unique design to produce comparable radiation pattern of X-band and Ka-band. Thus, the transmitting and receiving gain near boresight has similar values for X-band (44.5 dBiL and 43 dBiL) and Ka-band (47.5 dBiL and 47 dBiL). The dBiL value refers to gain (dB) relative to an isotopic linearly polarized antenna (Mukai, Ryan, 2017).

The HGA employs a right-hand circular polarization (RHCP) for downlink and left-hand circular polarization (LHCP) for uplink at Ka-band and RHCP for both downlink and uplink at X-band. The different circular polarization ensures avoidance of a mutual interference, thus more communication paths. Also, during the EFB, different polarization on a receiver and transmitted attenuates an unncessarily strong signal for such short distance. A circularly polarized signal either right-hand or left-hand prevents a signal degradation due to atmospheric conditions and omits the Faraday effect.

Moreover, the antenna cannot operate at RHCP and LHCP simultaneously, therefore a polarizer must be employed to switch between the polarizations. The CP efficiency is determined by an axial ratio and a cross-polarization. The axial ratio is the difference in amplitudes of two orthogonal E-field components (equal amplitudes result in 0 dB loss). Especially crucial is to maintain the axial ratio of the X-band uplink < 2.0 dB, such condition is met with 1.42 dB axial ratio for given path. The cross-polarization represents undesirable circulation in the opposite direction than intended as no signal can be polarized in one direction with 100%. Cause of such phenomena is in the polarization discrepancy between the feed antenna and subreflector. The cross-polarization is minimized beyond disturbance by the design of the involved antenna elements. (Vacchione, et. al, 2017)

The beamwidth of 0.25 degrees from boresight requires accurate Earth-pointing, hence the implementation of spinning spacecraft. Additionally, due to frequency differences, the X-band possesses 4 times the beamwidth compared to Ka-band, however this does not imply any problem.

4.2.1.2 Medium Gain Antenna (MGA)

The MGA is a conical horn type antenna located on the fore of the spacecraft adjacent to the HGA rim mounted on a separate easel. The antenna is additionally attached to a mechanical support, which provides flexibility when not directly pointing to Earth. The required 10.3° beamwidth near boresight for uplink and 9.3° for is achieved by adjusting the horn's length, resulting in the beamwidth wider than the HGA's and narrower than the LGAs'. Employement of two polarizers for the RHCP and LHCP provides additional means of communication in case of malfunction with sufficient gain of approximately 18.5 dBiC for uplink as well as downlink. (Vacchione, et. al, 2017)

4.2.1.3 Forward and Aft Low-Gain Antennas (FLGA and ALGA)

The omnidirectional FLGA and ALGA share same choke horn design and parameters with the only exception of one being mounted on the aft and the other on the fore of the spacecraft. This arrangement is used for communication during the Earth approach and subsequent departure. Similarly, to the MGA, both low gain antennas utilize a mechanical support for slight adjustments in the pointing, although having the highest beamwidth of the employed Telecom antennas of 41 degrees near boresight. This is due to the short operational window during the close Earth encounters. Furthermore, the antennas possess a low uplink 8.7 dB and downlink 7.7 dB gain because only short communication link is required. (Vacchione, et. al, 2017)

In addition to the antenna type, the choke horn allows to avert the multipath interference caused by processing signals from two or more propagation paths, which are each on its path altered by dissimilar types of reflection (e.g. mountains). The two antennas employ only the RHCP.

4.2.1.4 Toroidal Low-Gain Antenna (TLGA)

Unlike in the case of other Telecom antennas, by the design TLGA provides coverage of the spacecraft's blind spots, which serves crucial role in situations when the spacecraft points away from Earth during the DSM, JOI, and PRM. The biconical dipole antenna is used with 90 degrees tilt with respect to the spacecraft main axis, thus providing full spherical coverage.

To overcome considerable distance during the Jupiter Orbit Insertion, the TLGA produce uplink gain of 5.5 dBiC and downlink gain of 6.5. However, the gain is comparatively low, hence the TLGA is capable of sending only small portions of data, sufficient enough to remain in contact with Earth. (Vacchione, et. al, 2017)

4.2.2 X-band

4.2.2.1 Small Deep Space Transponder (SDST)

The SDSTs interconnect the Command & Data Handling Unit with the Telecom Subsystem and serves as an interface between them. Juno incorporates two configurations of the SDSTs. One is a redundant X-band receiver and X-band exciter (X/X configuration) and the latter a X-band receiver with X-band and Ka-band exciters (X/X/Ka). The Ka-band uplink is handled by the Ka-Band Translator. The X/X configuration can be in case of malfunction readily substituted by the X/X/Ka configuration, hence the redundancy. The SDST are further composed of the downconverter module, the digital processing module, the power converter module, and the exciter module.

The SDSTs acquire an uplink signal from a DSN modulated with a command data or ranging signal or both. The uplink signal is in the downconverter module converted into a lower intermediate frequency and subsequently digitalized at a rate of approximately 12.73 MHz. The sampling rate is derived from equation 4/3*F1, with F1 being the fundamental frequency 9.55 MHz. Then the signal proceeds to the digital processing module, which incorporates 3 channels. In the command channel, a command subcarrier is demodulated and send to the C&DH unit. Similarly, a ranging signal is demodulated from a signal and then directed to the D/A convertor for a downlink signal modulation with the turn-around ratio (749F1 uplink and 880F1 downlink). The carrier channel is facilitating the uplink carrier tracking through the phase lock loop. Additionally, the module processes a telemetry data from the C&DH and either directly modulates a carrier in case of higher bit rates or binary phase shift key (BPSK) modulates a square-wave subcarrier (with 25 kHz or 281.25 kHz) for lower bit rates. The exciter module phase modulates a downlink carrier with telemetry, differential one-way ranging (ΔDOR), and ranging. The Power converter module provides power to internal modules of the SDSTs.

4.2.2.2 Traveling Wave Tube Amplifier (TWTA)

The TWTA is employed as it can greatly amplify a fairly weak signal. Furthermore, helix type of the two TWTAs is used for it requires low-power dc input of 56 W, which is crucial for such energy efficient spacecraft as is Juno. Moreover, the broadband (over 2 octaves) of the TWTAs readily covers entire X-band, while providing steady 25 W output. The TWTAs consists of amplifying traveling wave tube and power supplying electrical power converter.

Firstly, a modulated downlink signal is from either or both SDSTs fed through the passive quadrature hybrid coupler (HY1), which splits either one or two signals and produces two equally powered signals on the output. Only after that is the signal fed to the TWTA1 and TWTA2 inputs. A signal is amplified via interaction of radio waves and electron beam. A downlink signal (radio wave) is propagated through a helix coil wired around an electron beam (both in the same direction) generated by an electron gun. As a result of the mutual interaction, signal's velocity is gradually decreased, thus amplified (TWT Theory of Operation).

4.2.2.3 X-Band Diplexer (DX) and Isolator (Iso)

The DX is another passive device providing a frequency division multiplexing, which allows transmission of separate signals over a single communication medium (Wikipedia). the DX consists of three ports. The two ports (left and bottom port in the Figure 6) are dedicated for the uplink (Rx) and downlink (Tx) signal, while the third facilitates transmission of both signals.

The Isolators are also passive devices placed after the TWTAs and before the DXs. It is a non-reciprocal device conducting a signal to a next port in a direction of rotation. A signal acquired from the TWTAs is transmitted in direction of rotation to the DXs inputs. However, a signal coming from the DXs would be absorbed as a next port in a

direction of rotation is the termination port. This one-way conductivity ensures that in case of a error in the DXs no downlink signal enters an uplink transmission line.

4.2.2.4 Waveguide Transfer Switch (WTS)

The WTSes are passive devices implemented to divert an uplink or downlink signal to or from the engaged antennas with low insertion loss of 0.05 dB. As Figure 6 illustrates, WTS1 and WTS2 takes output of the DX1 and DX2 and redirects it to either the MGA or other the WTSes (numbers 3,4, and 5), which further forwards the signal to the remaining antennas. X-band downlink travels through the waveguide type WR112. The number 112 refers to the waveguide bandwidth, which is this case X-band. 1the WR28 and WR34 facilitates higher Ka-band frequencies, in case of the WR28 it is 25.5 GHz to 40 GHz, whereas for the WR34 it is only 22 GHz to 33 GHz. The Waveguide's are employed because they provide low-loss and high insulation, which is essential for high-gain signals.

4.2.3 Ka-Band

4.2.3.1 Ka-Band Translator (KaTS)

The Ka-TS is Ka-band equivalent of the X-band SDSTs implemented for the Gravity Science investigation, the gravity doppler tracking in particular. A received uplink carrier with 34 GHz is through the turn around ratio of 3360/3599 for Ka-band translated to a downlink carrier with 32 GHz. Furthermore, the downlink signal is amplified at the Solid State Power amplifier by +34 dB (Mukai, Ryan, 2017). Additionally, the low-pass filter (LPF1) is implemented in the downlink path to cut-off any frequencies higher than intended, while in the uplink path is incorporated the band-pass filter (BPS1), which lets through only frequencies centered around 34GHz.

5. SPACECRAFT'S SCIENTIFIC INSTRUMENTS

Scientific payload of the Juno spacecraft comprises of nine instruments with unique tasks to measure various properties of the Jupiter system and are specially designed to endure in its harmful environment.

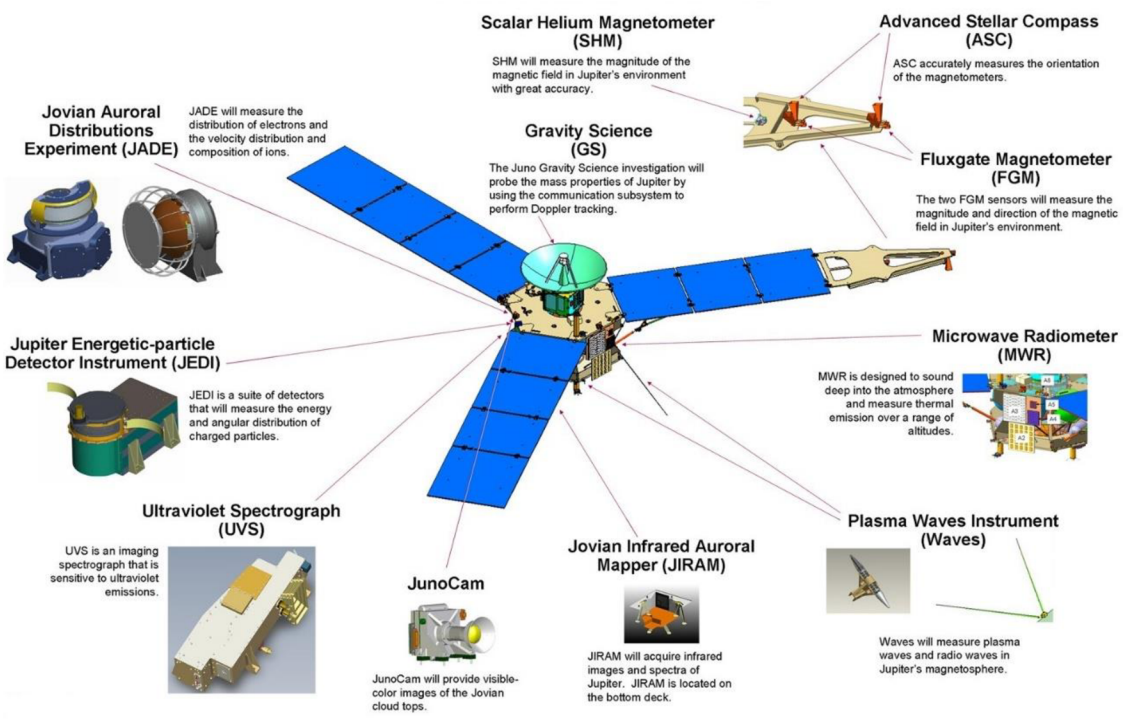

Figure 8 The scientific payload of the Juno spacecraft

5.1 Gravity science – GS

The Gravity science (GS) experiment consists of the DSN's X-band and K_a-band telecommunication systems and the Juno's high-gain antenna and X-band and K_a-band transponders. The GS is a measurement of Jupiter's gravitational field, which is essential for a better understanding of the interior structure of the planet. It is determined by the measurements of Doppler shift, which is defined as a change of frequency emitted by a

source, which is moving relative to an observer. Firstly, a signal tone is sent from Earth's DSN (uplink) to the Juno's spacecraft then is mirrored on the spacecraft back to the DSN (downlink). The signal tone is recorded and calibrated because the signal encounters sources of delays on its way to the DSN, e.g. spacecraft's and station's electronics, interplanetary plasma, atmosphere, and ionosphere (Asmar, 2017). Lastly, the data are used to determine the velocity as a function of time with an accuracy of 1 meter.

5.2 Magnetometer – MAG

The magnetic field of Jupiter was already observed by various spacecraft and the Juno's goal is to map the magnetic field, determine the dynamics of Jupiter's interior, and the three-dimensional structure of the polar magnetosphere and its auroras (Juno Magnetic Field Investigation, 2017). Jupiter's findings will help us determine the nature of Jupiter's core and how is its magnetic field generated.

The magnetic field experiment consists of two magnetometer sensor suites. Each contains the Advanced Stellar Compass (ASC) and Fluxgate Magnetometer (FGM).
The ASC and FGM are installed on the 3,6 metres long magnetometer boom, which is affixed to the outer end of one of the 9-metres-long solar array panels, to avoid magnetic interferences from the spacecraft.

5.2.1 Advanced Stellar Compass

The ASC is a star tracker that contains a Data Processing Unit and CCD cameras. The camera takes pictures of a stellar space and compares it in the data processing unit with the stellar map database uploaded in the computer to determine the orientation of the spacecraft.

5.2.2 Fluxgate Magnetometer

The FGM comprises of a triaxial scalar-helium-magnetometer sensor and a dual-fluxgate magnetometers to measure a magnetic field vector and a strength of the magnetic field. The fluxgate magnetometers are attached at different distances. One of them is in the middle and the latter at the end of the magnetometer boom. They determine and subtract the magnetic influence of the main body of the spacecraft.

To avoid the intense radiation environment of the planet, Juno must fly in highly elliptical orbits. These elliptical orbits lead the spacecraft through the space between the planet and the most intense radiation belts. It had been determined 33 close-in polar orbits to equally map the magnetosphere. Each with longitude separation of 12° for it must be accurate and low-energy-cost with minimal exposure to the radiation environment.

5.3 Microwave Radiometer – MWR

MWR is a set of devices that utilizes six antennas with dissimilar wavelengths (see Table 1) to study different regions of Jupiter's atmosphere. Antennas are attached to the outside of the spacecraft body and the radiation-sensitive technology: the receivers and electronics subsystem is hidden inside the radiation vault to ensure their accuracy and reliability.

Table 1 Microwave Radiometer antennas properties

Antenna	Design	Frequency [Ghz]	Wavelength [cm]	Range [K]	Bandwidth [%]	Beamwidth [deg]
A1	patch array	0.6	50	0-1000	3.50	20.6°
A2	patch array	1.248	24	0-800	3.51	21°
A3	slot array	2.597	11.55	0-700	3.25	12.1°
A4	slot array	5.215	5.75	0-600	3.24	12.1°
A5	slot array	10.004	3.0	0-400	3.25	12.0°
A6	Corrugated horn	21.900	1.37	0-300	3.52	10.8°

5.3.1 Antennas

The spacecraft is equipped with six specially constructed antennas with various properties, thus allowing to focus on certain aspects of each antenna. All six antennas are mounted on the metal plates with neglection of dielectrics, therefore providing additional properties, e.g. low mass, wide bandwidth, and good thermal and emissivity properties.

The A1 is designed to peek into the deepest parts of the planet up to 550km. Thus it possesses the lowest frequency and the longest wavelength to penetrate the ammonia clouds. The beamwidth of 20° is sufficiently achieved by 5x5 patch array and due to its large proportion is attached to the other side of the spacecraft body than the other antennas. The A2 is compared to the A1 quarter of its size with almost similar properties expect frequency and wavelength, which vary significantly. The A3-A5 are antennas of slot array design to achieve low sidelobes (narrower angle of the beamwidth) and higher spatial resolution while keeping the low mass. A6 is a corrugated horn, which provides the highest frequency with sufficient beamwidth and exceptionally low sidelobes. To maintain the low mass the horn is profile shaped.

5.3.2 Receivers subsystem

Receivers subsystem was derived from the Advanced Microwave Radiometer (AMR) Ocean Surface Topography Mission (OSTM) from 2008. The subsystem consists of a six Dicke-switched radiometers in a direct-detection design with dynamic range for each channel determined as a minimum of two times the anticipated maximum antenna temperature from the planet. Out-of-band signal rejection of the bandpass along with the 4% radio frequency passband width is provided by the two-staged microstrip bandpass filters, which matches the antenna passbands. Diode detector enables conversion of the radiofrequency signal to DC and the converted data then further proceeds to video amplification.

5.3.3 Sensors

The wave sensors consist of a magnetic search coil for measurement of magnetic components and a v-shaped electrical dipole antenna for measurement of electrical fields. The antenna's tip-to-tip length is 4.8 meters and is attached aft of the solar array panel to be symmetrical with the magnetometer boom extension. The antenna is capable of detecting electric fields frequencies from 50 Hz to 40 MHz. The Magnetic search coil (MSC) is mounted underneath the flight deck perpendicular to the spacecraft spin axis and the solar array panels to reduce the influence of the spin-modulated planetary field of Jupiter (Janssen, 2017).

The Magnetic coil is made of a 15 cm long mu-metal core with 10,000 turns of copper wire. The length and material of the core provide high magnetic permeability. Hence the magnetometer system is not influenced by the induced magnetic field. The magnetic search coil is designed to detect magnetic fields in the frequency range of 50 Hz to 20 MHz.

5.3.4 Receivers

The frequency range of 50 Hz – 40 MHz is covered with the high-frequency receiver (HFR) and the low-frequency receiver (LFR).

The LFR comprises of three channels. The first two are identical and designed with two configurations for frequencies from 50 Hz to 20 kHz. In the first configuration channels simultaneously analyse plasma waves detected by the electrical and magnetic sensors and sample the data. In the second configuration is used the first channel in a noise-cancelling mode and detected electrical and magnetic fields are analysed in the second channel. The third channel is used for higher frequencies (10 kHz to 150 kHz) and electrical signals.

The HFR consists of two nearly identical receivers. One is devised as a spectrum analyser for spectrum compilation of frequencies between 100 kHz and 3 MHz from digital spectrum analysis, whereas the latter is a swept frequency receiver for 3 to 40 MHz frequencies that detect the amplitude of signals in 1-MHz bandwidths.

5.3.5 Data Processing Unit

The Data Procession Unit (DPU) processes outputs of the receivers and comprises of two processors with field-programmable gate array (FPGA) and system on chip design. Their task is data housekeeping and storage, onboard analyses, applying digital signal processing tasks (Fourier transforms), and data compression and formatting.

5.4 Ultraviolet Spectrograph – UVS

The UVS instrument is capable of observation of both the extreme-ultraviolet (124 nm–10 nm) and far-ultraviolet (68–210 nm) spectral range, hence allows an analysis of

the prime UV emissions of the auroral regions with 125 km resolution. Additionally, the spectrograph is designed to execute in-situ measurements.

The UVS is comprised of a telescope/spectrograph assembly and vault electronics box. The spectrograph is composed of a series of components that process a signal. The off-axis Primary Mirror focuses detected light, on an entrance slit in three adjacent 2° sections of 0.2°, 0.05°, and 0.2°, without causing a spherical aberration. The light is then dissipated by a toroidal grating onto a curved microchannel plate (MCP) with a cross delay line (XDL) detector to be processed by the detector electronics (Gladstone, 2017). The vault electronics box, which executes all the in-situ measurements, is shielded in the titanium vault along with the other vulnerable electronics.

5.5 Jupiter Energetic Particle Detector Instrument – JEDI

The JEDI is implemented to study the magnetosphere, particularly the auroras of the polar space environment, to understand a root cause and a process of a generation of the auroras. The JEDI analyses the energy, angular, and compositional distribution of the detected ions within an energetic range of 20 keV – 1 MeV for Hydrogen and 50 keV – 1 MeV for Oxygen and the electrons within an energetic range of 40 – 500 keV. Also, JEDI operates in coordination with JADE.

The JEDI is a suite of three nearly identical detectors. Each incorporates sensor head and electronics. The sensor further comprises an ion and electron sensor, and preamplifier.

5.6 Jovian Auroral Dynamics Experiment – JADE

JADE instruments are similar to the JEDI ones. It is a set of instruments for measurement of low energy electrons and ions that produce auroras in Jupiter magnetosphere. The instrument suite consists of the JADE-E, the JADE-I, and the Electronics Box.

The three identical JADE-E sensors are aligned on the bottom of the flight deck in a manner to achieve a 360° field of view (120°each). JADE-Es focus on measurement of electrons pitch-angle within an energetic range of 0.1 to 100 keV. Furthermore, the suite contains lower and upper deflectors for electron deflection and a micro-channel plate detector.

The JADE-I is close to its function and design to the JADE-Es. However, it measures ions instead of electrons, particularly the ions composition of the magnetosphere plasma within the energetic range of 10 eV to 45 keV. Although its field of view is only 270 x 90, thanks to the spacecraft rotation the instrument can observe all direction once every 30 seconds as Juno rotates with 2RPM.

The Electronics box is hidden inside the Radiation vault to be protected against the radiation of Jupiter and provides in situ analyses of measured data from the both JADE sensors.

5.7 Jovian Infrared Auroral Mapper – JIRAM

The JIRAM obtains images in two infrared bands. The 2-3 μm band observes atmospheric compounds such as water (H_2O), ammonia (NH_3), and phosphine (PH_3). On the other hand, the 4-5 μm band observes auroral and non-auroral emissions (H_3^+), and thermal emissions in the atmosphere. Apart from that, the instrument can also study Galilean moons.

The instrument comprises of a telescope that incorporates the imager (IMG) with 2-3 μm band and the spectrometer (SPE) with 4-5 μm band channel, and a despinning flat mirror for compensation of the rotation of the spacecraft.

5.8 JunoCam

JunoCam takes pictures in filter strips as the spacecraft spins with a resolution of 1600x155 pixels. The camera uses 2 types of filters: RGB filter in the visible light

spectrum for full-colour images and methane filter in the infrared spectrum to determine methane abundance (Image processing gallery).

The JunoCam's other purpose is public outreach. Amateur astronomers can share their images and data of Jupiter to provide background for the JunoCam images. Additionally, people can process the images taken by the JunoCam with NASA's free software and send them back.

6. PRELIMINARY RESULTS OF THE JUNO MISSION AS OF MAY 2020

By the May 2020, Juno completed the 25th perijove with 9 perijoves ahead before the planned end of the mission on July 2021. Since the Juno mission is not finished, some of the major objectives have not been accomplished, such as what type of core Jupiter possesses. Therefore, the results presented in this chapter are based only on the hitherto completed perijoves and gathred data.

Regarding the future exploration of Jovian system, there are two missions scheduled. The Europa clipper is planned to launch in 2024 with the aim to study Europa a Galilean moon of Jupiter. The latter mission is called Io Volcano Observer set to launch between the years 2026 and 2028 and implement to study other Galilean moon Io. Since the both missions are going to operate in close distance from Jupiter. Studying the gas giant may be a minor objective of their mission.

6.1 Gravitational Field

Data acquired by the GS show a north-south (hemispheric) asymmetry in the gravity field of the planet. Atmospheric dynamics, which are represented by the differential rotation (uneven angular velocity of zones and belts) and deep atmospheric flows. These density perturbations along with the predominant axial and hemispherical symmetry produced by the planets rotation results in Jupiter's complex gravitational field (Iess, Folkner, 2018).

Data from the measurement of gravity field also shows that the core is not concentrated in the very centre of the planet, as it is in case of Earth. Instead, the data shows the core might be half the size of the planet. *"There may be a core there, but it's very big, and it may be partially dissolved. We're studying that, but that came as a big surprise to us that there was no core."* (Scott Bolton, 2017). The new model suggests that

the planet has diluted core with a size of half the planet and comprised of heavy elements (Liu, 2019).

6.2 Magnetic Field

First observation shows that Jupiter's magnetosphere is much stronger than anticipated with uneven distribution. When compared to previous missions, Jupiter's new magnetic field model (JRM09) shows magnetic field changing in time, such phenomenon is called secular variation (The Daily Galaxy, 2019). Cause of the changes in the magnetic field can be the Great Blue Spot (represented by the dark blue spot in the Figure 9) and the cloud-level zonal winds. The confined magnetic field of the Great Blue Spot with strong zonal winds affect the magnetic field of the whole planet and its dynamics with implication on the interior structure and possibly the core revelation.

Further study of the Juno's magnetic field indicates the field is not generated in a simple homogenous region. Meaning the magnetic field is predominantly non-dipolar in the northern hemisphere and dipolar on the southern hemisphere, for example, Earth is primarily dipolar. This can be caused by the drift of liquid metallic hydrogen in its interior (Tsang). Under the harsh Jupiter's interior environment, hydrogen gas changes to fluid with metal-like conductivity (liquid metallic hydrogen), which surrounds Jupiter's dynamo. However, above the layered-liquid-metallic-hydrogen region is a steep gradient in electrical conductivity due to which it was not possible to observe at what depth dynamo's actions become significant to determine its properties (Moore, 2018). Thus, further investigation is needed.

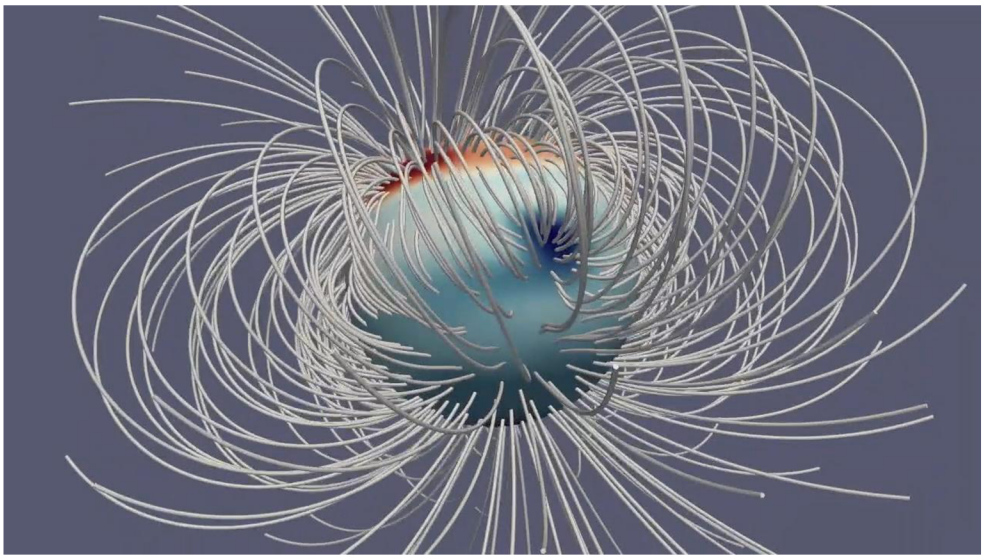

Figure 9 Magnetic field of Jupiter. Field lines represent direction of the magnetic field in space, while the strength of the field is representend by the deepness of the color with red being positive and blue negative.

6.3 Polar Regions

Upon the Juno's observation, it seems as the auroras are not created the same way as on Earth, by the charged particles interacting with field lines (field lines are illustrated in Figure 9). Early assumptions suggest they are rather created by the particles surging out of the Jupiter's atmosphere. The particles are increasingly accelerated to a wide range of energies, such phenomenon is called turbulent acceleration. The particles are captured by the plasma wave above the Jupiter's atmosphere, as they emerge from the planet. The interaction of various plasma waves at the polar regions with particles of a different energetic level creates Jupiter's auroras. However, the origin of the emerged particles is unknown, and more research is needed for this hypothesis to be proven (Mauk, Haggerty, 2016).

6.4 Atmospheric Dynamics and Interior Structure

In addition to the differential rotation, the investigation indicates that such phenomenon is suppressed deep in the planets interior. The zonal winds (driving force of the atmospheric dynamics) cannot persist in the depths around 2,000 to 3,500 kilometres below the cloud tops and slowly decays up to those depths. This indicates interior rotation of a rigid body as at the mentioned depths a magnetic drag–product of electrical conductivity–becomes a considerable factor acting against the differential rotation, thus suppressing it. (Guillot, Miguel, 2018)

The deep interior flows, a probable source of the hemispherical asymmetry, are composed of the jet streams at the cloud-top layer (see Figure 10) extending deep into the planets interior. The jet streams may be composed of a mass equal to the 1 percent of the total mass of Jupiter (Kaspi, Galanti, 2018).

6.5 Ammonia and Water Abundance

A probing of Jupiter's atmosphere layers reveals (up to the depth of 350 km) its non-uniform composition, particularly ammonia distribution. Jupiter possesses a belt of ammonia at its equator that probably expands beyond the detection limits of the Juno's instruments (A Whole New Jupiter: First Science Results from NASA's Juno Mission, 2017). Furthermore, at a depth of 200 km and lower the ammonia concentration is higher than at the outer layer.

Juno searched for traces of water molecules around the equator area for it may indicate accurate global distribution of the H_2O. Similar measurement did the Galileo probe, revealing the lesser amount of water components compared to the Sun. However, data were taken from the depth of 120 km at one location, which may not apply to the planetwide distribution. But more importantly, the probe was destroyed by the environment before finishing the measurement. For this reasons, Juno water abundance

measurement is highly anticipated. The MWR instruments peered 150 km (33 bars) deep in to the atmosphere revailing 0.25 % concetration of water molecules with implaction on planets origin and meteorology (Findings From NASA's Juno Update Jupiter Water Mystery)

6.6 Images of Jupiter

During every orbit, the spacecraft takes images of the planet in unprecedented detail. The images revealed a blue colour of polar regions. In addition to this, were discovered cyclone storms on both poles (Wall, 2019). The Figure 10 was taken during the perijove 25 on February 17, 2020.

Figure 10 JunoCam image of the southern hemisphere. The equatorial band of different altitude and color represents zonal atmospheric flows, also called jet streams.

CONCLUSION

There have been many spacecrafts in the last 50 years that studied Jupiter and its surroundings, but none of them had advantages of the Juno spacecraft. With the state-of-the-art technologies the Juno mission was send to Jupiter and determine–through the measurement of its primary objectives– type of the planet's core, thus the origin and evolution of the planet and the Solar System in general.

Albeit, the Juno mission have not delivered conclusive results about Jupiter's core, the mission is far from over. There are several perijoves left for the Juno to gather necessary data, which will be studied long after the spacecraft planned dove into the planet, which brings its end. Moreover, more missions to Jovian System are scheduled, which may contribute to the findings of the Juno mission.

Even though the bigger questions are still remaining unanswered, the mission have been successful in mapping Jupiter's magnetosphere reveiling the Great Blue Spot responsible for the secular variation of the magnetic field. Juno also mapped the gravity field of Jupiter, which shows the north-south asymmetry, probably caused by jet streams. Along with the water abundance measurement and the spacecraft's splendid images of Jupiter, the mission have already fulfill its expactations, when it managed to endure such unfriendly environment as Jupiter has for so logn. The mission set new bounderies, or rather frontiers, of our understanding of the world around us, by exploring the least known world in our Solar System.

LIST OF TABLES

JANSSEN, M.A., J.E. OSWALD a J.E. BROWN. MWR: Microwave Radiometer for the Juno Mission to Jupiter. *Space Science Reviews*. Springer Netherlands, 2017, 2017(213), 139–185. DOI: 10.1007/s11214-017-0349-5. ISSN 0038-6308. Retrieved from: https://link.springer.com/article/10.1007/s11214-017-0349-5

LIST OF FIGURES

Juno Mission & Trajectory Design: Launch. Spaceflight101: Space News and Beyond [online]. [cit. 2020-05-31]. Dostupné z: https://spaceflight101.com/juno/juno-mission-trajectory-design/

MUKAI, Ryan, David HANSEN, Anthony MITTSKUS, Jim TAYLOR, Monika DANOS a Andrew KWOK, HAMKINS, Jon, ed. Design & Performance Summary Series: Juno Telecommunication. Jet Propulsion Laboratory, California Institute of Technology: Deep Space Communications and Navigation Systems Center of Excellence, 2017.

BOLTON, S. J., J. LUNINE, D. STEVENSON, et al. The Juno Mission. Space Science Reviews. 2017, 213(1-4), 5-37. DOI: 10.1007/s11214-017-0429-6. ISSN 0038-6308. Dostupné také z: http://link.springer.com/10.1007/s11214-017-0429-6

DAWSON, Stephen, Paul STELLA, William MCALPINE a Brian SMITH. Juno Photovoltaic Power at Jupiter. 4800 Oak Grove Drive, Pasadena, CA 91109.

ASMAR, Sami W., Scott J. BOLTON, Dustin R. BUCCINO, et al. The Juno Gravity Science Instrument. Space Science Reviews. 4800 Oak Grove Drive, Pasadena, CA 91109, 2017, 213(1-4), 205-218. DOI: 10.1007/s11214-017-0428-7. ISSN 0038-6308. Dostupné také z: http://link.springer.com/10.1007/s11214-017-0428-7

MUKAI, Ryan, David HANSEN, Anthony MITTSKUS, Jim TAYLOR, Monika DANOS a Andrew KWOK, HAMKINS, Jon, ed. Design & Performance Summary Series: Juno Telecommunication. Jet Propulsion Laboratory, California Institute of Technology: Deep Space Communications and Navigation Systems Center of Excellence, 2017.

Juno Spacecraft: Communication system. Mission Juno [online]. San Antonio, Texas, USA: Southwest Research Institute [cit. 2020-05-11]. Dostupné z: https://www.missionjuno.swri.edu/spacecraft/juno-spacecraft

Sonda Juno. Malá encyklopedie kosmonautiky [online]. [cit. 2020-06-08]. Dostupné z: https://mek.kosmo.cz/sondy/usa/juno/index.htm

LIST OF REFERENCES

SIDDIQI, Asif A. *Beyond Earth: A Chronicle of Deep Space Exploration, 1958-2016.* National Aeronautics and Space Administration, Office of Communications, NASA History Division, 2018. ISBN 9781626830431.

DUNBAR, Brian, ed. *The Pioneer Missions* [online]. National Aeronautics and Space Administration, March 26, 2007 [cit. 2019-12-17]. Dostupné z: https://www.nasa.gov/centers/ames/missions/archive/pioneer.html

MARS, Kelli, ed. *45 Years Ago, Pioneer 10 First to Explore Jupiter* [online]. National Aeronautics and Space Administration, 2018, Dec. 3 [cit. 2019-12-17]. Retrieved from: https://www.nasa.gov/feature/45-years-ago-pioneer-10-first-to-explore-jupiter

Voyager - Mission Timeline [online]. National Aeronautics and Space Administration [cit. 2019-12-17]. Retrieved from: https://voyager.jpl.nasa.gov/mission/timeline/

BARRETT, Mike, ed. *The Jovian System* [online]. RocketStem, 2016, August 15 [cit. 2019-12-17]. Retrieved from: https://www.rocketstem.org/2016/08/15/the-jovian-system-factlets/

Galileo Mission [online]. National Aeronautics and Space Administration [cit. 2019-12-17]. Retrieved from: https://solarsystem.nasa.gov/missions/galileo/overview/

BELL, II, Dr. Edwin V. *Galileo Project Information* [online]. Mail Code 690.1: NASA Goddard Space Flight Center, 1996, May 3 [cit. 2019-12-17]. Retrieved from: https://nssdc.gsfc.nasa.gov/planetary/galileo.html

Mission to Jupiter: Galileo [online]. National Aeronautics and Space Administration [cit. 2019-12-17]. Retrieved from: https://www.jpl.nasa.gov/missions/galileo/

GREICIUS, Tony, ed. *Juno: Juno Armored Up to Go to Jupiter* [online]. National Aeronautics and Space Administration, 2010, January 7 [cit. 2019-12-17]. Retrieved from: https://www.nasa.gov/mission_pages/juno/news/juno20100712.html

Press kit: Juno spacecraft [online]. National Aeronautics and Space Administration [cit. 2019-12-17]. Retrieved from: https://www.jpl.nasa.gov/news/press_kits/juno/spacecraft/

Press kit: Juno spacecraft [online]. National Aeronautics and Space Administration [cit. 2019-12-17]. Retrieved from: https://www.jpl.nasa.gov/news/press_kits/juno/overview/

Juno Spacecraft and Instruments [online]. National Aeronautics and Space Administration, 2015, March 13 [cit. 2019-12-17]. Retrieved from: https://www.nasa.gov/mission_pages/juno/spacecraft/index.html

HOWELL, Elizabeth. *Juno is Powered by the Sun, and That's a Big Deal: Solar panels for the outer solar system.* [online]. National Aeronautics and Space Administration, 2016, July 5 [cit. 2019-12-17]. Retrieved from: https://www.airspacemag.com/space/juno-powered-sun-and-s-big-deal-180959691/

BRAKELS, Ronald. *Solar Innovations: Why NASA Chose Solar Power Over Nuclear For The Juno Space Probe* [online]. 2016, July 6 [cit. 2019-12-17]. Retrieved from: https://www.solarquotes.com.au/blog/nasa-chose-solar-power-nuclear-juno-space-probe/

PATRICK, Blau. *Spacecraft Information* [online]. [cit. 2019-12-17]. Retrieved from: http://spaceflight101.com/juno/spacecraft-information/

Juno Solar Panels Complete Testing: Juno Mission Status Report [online]. 2011, May 27 [cit. 2019-12-17]. Retrieved from: https://www.nasa.gov/mission_pages/juno/news/juno20110527.html

WALL, Mike. *Juno Probe Will Run Hellish Radiation Gauntlet at Jupiter Monday* [online]. 2016, July 02 [cit. 2019-12-17]. Retrieved from: https://www.nasa.gov/mission_pages/juno/news/juno20110527.html

GOUGH, Evan. *Juno and the Deep Space Network: Bringing The Data Home* [online]. 2016, June 30 [cit. 2019-12-17]. Retrieved from: https://www.universetoday.com/129636/juno-and-the-deep-space-network-bringing-the-data-home/

BLAU, Patrick. *Juno Instrument Overview* [online]. [cit. 2019-12-17]. Retrieved from: http://spaceflight101.com/juno/instrument-overview/

HELLED, Ravit a Jonathan LUNINE. Measuring Jupiter's water abundance by Juno: the link between interior and formation models. *Monthly Notices of the Royal Astronomical Society* [online]. Oxford University Press, 1 July 2014, (Volume 441, 3,), 2273–2279 [cit. 2019-12-18]. DOI: https://doi.org/10.1093/mnras/stu516. ISSN 0035-8711. Retrieved from: https://academic.oup.com/mnras/article/441/3/2273/1105754

Juno Magnetic Field Investigation [online]. National Aeronautics and Space Administration, 2017 [cit. 2019-12-18]. Retrieved from: https://junomag.gsfc.nasa.gov/

ASMAR, S.W., S.J. BOLTON a D.R. BUCCINO. The Juno Gravity Science Instrument. *Space Science Reviews* [online]. Springer Netherlands, 25 October 2017, 2017, 205–218 [cit. 2019-12-18]. DOI: 10.1007/s11214-017-0428-7. ISSN 1572-9672. Retrieved from: https://link.springer.com/article/10.1007%2Fs11214-017-0428-7

CONNERNEY, J.E.P. a M. BENN. The Juno Gravity Science Instrument. *Space Science Reviews*. Springer Netherlands,2017, 2017, (213), 205-218. DOI: 10.1007/s11214-017-0428-7. ISSN 0038-6308. Retrieved from: https://link.springer.com/article/10.1007%2Fs11214-017-0428-7

JØRGENSEN, John Leif, ANDERSEN, Morten Garly, ed. Stellar navigation. *DTU Space: National Space Institute* [online]. [cit. 2019-12-18]. Retrieved from: https://www.space.dtu.dk/english/Research/Instruments_Systems_Methods/Stellar navigation

JANSSEN, M.A., J.E. OSWALD a J.E. BROWN. MWR: Microwave Radiometer for the Juno Mission to Jupiter. *Space Science Reviews*. Springer Netherlands, 2017, 2017(213), 139–185. DOI: 10.1007/s11214-017-0349-5. ISSN 0038-6308. Retrieved from: https://link.springer.com/article/10.1007/s11214-017-0349-5

CHAMBERLAIN, N., J. CHEN, R. HODGES, R. HUGHES a J. JAKOBOSKI. Juno microwave radiometer all-metal patch array antennas. *IEEE Antennas and Propagation Society International Symposium* [online]. Toronto, Canada, 2010, , 1-4 [cit. 2019-12-18]. DOI: 10.1109/APS.2010.5561183. ISSN 1947-1491. Retrieved from: http://ieeexplore.ieee.org/stamp/stamp.jsp?tp=&arnumber=5561183&isnumber=5560891

KURTH, W.S., G.B. HOSPODARSKY a D.L. KIRCHNER. The Juno Waves Investigation. *Space Science Reviews* [online]. Springer Netherlands, 2017, 10 July 2017, 2017(213), 347–392 [cit. 2019-12-18]. DOI: 10.1007/s11214-017-0396-y. ISSN 0038-6308. Retrieved from: https://link.springer.com/article/10.1007/s11214-017-0396-y

GLADSTONE, G.R., S.C. PERSYN a J.S. ETERNO. The Ultraviolet Spectrograph on NASA's Juno Mission. *Space Science Reviews* [online]. Springer Netherlands, 2017, 25 March 2014, 2017(213), 447–473 [cit. 2019-12-18]. DOI: 10.1007/s11214-014-0040-z. ISSN 0038-6308. Retrieved from: https://link.springer.com/article/10.1007/s11214-014-0040-z

MAUK, B.H., D.K. HAGGERTY a S.E. JASKULEK. The Jupiter Energetic Particle Detector Instrument (JEDI) Investigation for the Juno Mission. *Space Science Reviews* [online]. Springer Netherlands, 26 November 2013, 2017(213), 289–346 [cit. 2019-12-18]. DOI: 10.1007/s11214-013-0025-3. ISSN 0038-6308. Retrieved from: https://link.springer.com/article/10.1007/s11214-014-0040-z

MAUK, B. H., D. K. HAGGERTY, C. PARANICAS, et al. Juno observations of energetic charged particles over Jupiter's polar regions: Analysis of monodirectional and bidirectional electron beams. Geophysical Research Letters. 2017, 44(10), 4410-4418. DOI: 10.1002/2016GL072286. ISSN 00948276. Dostupné také z: http://doi.wiley.com/10.1002/2016GL072286

MCCOMAS, D.J., N. ALEXANDER a F. ALLEGRINI. The Jovian Auroral Distributions Experiment (JADE) on the Juno Mission to Jupiter. *Space Science Reviews* [online]. Springer Netherlands, 25 May 2013, 2017(213), 547–643 [cit. 2019-12-18]. DOI: 10.1007/s11214-013-9990-9. ISSN 0038-6308. Retrieved from: https://link.springer.com/article/10.1007/s11214-013-9990-9

JÓNSSON, Björn, ed. Diving into Juno JIRAM data archives. *The Planetary society* [online]. 11 April 2018 [cit. 2019-12-18]. Retrieved from: https://www.planetary.org/blogs/guest-blogs/2018/0411-diving-into-juno-jiram-data.html

JÓNSSON, Björn, ed. JIRAM. *PDS: The Planetery Atmospheres Node* [online]. National Aeronautics and Space Administration [cit. 2019-12-18]. Retrieved from: https://pds-atmospheres.nmsu.edu/data_and_services/atmospheres_data/JUNO/jiram.html

ADRIANI, A., G. FILACCHIONE a T. DI IORIO. JIRAM, the Jovian Infrared Auroral Mapper. *Space Science Reviews* [online]. Springer Netherlands, 1 October 2014, 2017(213), 393–446 [cit. 2019-12-18]. DOI: 10.1007/s11214-014-0094-y. ISSN 0038-6308. Retrieved from: https://link.springer.com/article/10.1007/s11214-013-9990-9

IMAGE PROCESSING GALLERY: About JunoCam Images [online]. National Aeronautics and Space Administration [cit. 2019-12-18]. Retrieved from: https://www.missionjuno.swri.edu/junocam/processing

Juno: Mission Overview [online]. National Aeronautics and Space Administration [cit. 2019-12-18]. Retrieved from: https://www.jpl.nasa.gov/news/press_kits/juno/overview/

BOLTON, Scott. PSW Science: Juno's Exploration of Jupiter. In: *Youtube* [online]. 2017, January 6 [cit. 2019-12-18]. Retrieved from: https://www.youtube.com/watch?v=af0oPFgx1Sw

What's In Jupiter's Core? *Mission Juno* [online]. [cit. 2019-12-18]. Retrieved from: https://www.missionjuno.swri.edu/origin?show=hs_origin_story_whats-in-jupiters-core

SCHUBERT, Gerald, Dali KONG a John D. ANDERSON. [online]. Proceedings of the National Academy of Sciences, 7 August 2018 [cit. 2019-12-18]. DOI: 10.1073/pnas.1805927115. ISSN 1091-6490. Retrieved from: https://www.pnas.org/content/115/34/8499/tab-article-info

"Jupiter's Great Blue Spot" --'Incredible! Impacts Its Entire Magnetic Field'. The Daily Galaxy [online]. 2019, 21 May [cit. 2019-12-18]. Retrieved from: https://dailygalaxy.com/2019/05/great-blue-spot-incredible-it-impacts-all-of-giant-jupiters-magnetic-field/

A Whole New Jupiter: First Science Results from NASA's Juno Mission. NASA [online]. 2017, 25 May [cit. 2019-12-18]. Retrieved from: https://www.nasa.gov/press-release/a-whole-new-jupiter-first-science-results-from-nasa-s-juno-mission

TSANG, Yue-Kin a Chris A. JONES, BUFFETT, B., ed. Characterising Jupiter's dynamo radius using its magnetic energy spectrum. Earth and Planetary Science Letters [online]. [cit. 2019-12-18]. DOI: 10.1016/j.epsl.2019.115879. Retrieved from: https://www.sciencedirect.com/science/article/pii/S0012821X19305710

MOORE, K.M., R.K. YADAV a L. KULOWSKI. A complex dynamo inferred from the hemispheric dichotomy of Jupiter’s magnetic field. *Nature* [online]. 2018, 05 September, (531), 76–78 [cit. 2019-12-18]. DOI: 10.1038/s41586-018-0468-5. Retrieved from: https://www.nature.com/articles/s41586-018-0468-5

LEIFERT, Leifert. Juno unveils Jupiter's secrets. Juno unveils Jupiter's secrets | EARTH Magazine [online]. 2019, March 11 [cit. 2019-12-18]. Retrieved from: https://www.earthmagazine.org/article/juno-unveils-jupiters-secrets

CONSTABLE, Catherine. NON-DIPOLE FIELD. Encyclopedia of Geomagnetism and Paleomagnetism [online]. 2005, July 7 [cit. 2019-12-18]. Retrieved from: https://www.earthmagazine.org/article/juno-unveils-jupiters-secrets

GREICIUS, Tony, ed. NASA's Juno Finds Changes in Jupiter's Magnetic Field. NASA [online]. 2019, 20 May [cit. 2019-12-18]. Retrieved from: https://www.nasa.gov/feature/jpl/nasas-juno-finds-changes-in-jupiters-magnetic-field

GREICIUS, Tony, ed. NASA Juno Findings - Jupiter's Jet-Streams Are Unearthly.

NASA [online]. 2018, 07 March [cit. 2019-12-18]. Retrieved from: https://www.nasa.gov/feature/jpl/nasa-juno-findings-jupiter-s-jet-streams-are-unearthly

LIU, S., Y. HORI a S. MÜLLER. The formation of Jupiter's diluted core by a giant impact. Nature [online]. 2019, 14 August, (572), 355–357 [cit. 2019-12-18]. DOI: 10.1038/s41586-019-1470-2. Retrieved from: https://www.nature.com/articles/s41586-019-1470-2

JOHNSON, T.V., L. COLIN, F.P. FANALE, L.A. FRANK a D.M. HUNTEN. Galileo: Exploration of Jupiter's System. 1985.

WALL, Mike. NASA Spacecraft Spies Huge New Storm on Jupiter After Death-Dodging Maneuver. Space [online]. 13 December 2019 [cit. 2019-12-19]. Retrieved from: https://www.space.com/nasa-juno-dodges-death-jupiter-polar-storm.html

BOLTON, S.J., J. LUNINE a D. STEVENSON. The Juno Mission. Space Science Reviews. Springer Netherlands, 2017(213), 5-37. ISSN 0038-6308.

Juno Spacecraft: Communication system. Mission Juno [online]. San Antonio, Texas, USA: Southwest Research Institute [cit. 2020-05-11]. Dostupné z: https://www.missionjuno.swri.edu/spacecraft/juno-spacecraft

MUKAI, Ryan, David HANSEN, Anthony MITTSKUS, Jim TAYLOR, Monika DANOS a Andrew KWOK, HAMKINS, Jon, ed. Design & Performance Summary Series: Juno Telecommunication. Jet Propulsion Laboratory, California Institute of Technology: Deep Space Communications and Navigation Systems Center of Excellence, 2017.

J. D. Vacchione, R. C. Kruid, A. Prata, L. R. Amaro and A. P. Mittskus, "Telecommunications antennas for the Juno Mission to Jupiter," 2012 IEEE Aerospace Conference, Big Sky, MT, 2012, pp. 1-16, doi: 10.1109/AERO.2012.6187091.

Deep Space Network: ABOUT THE DEEP SPACE NETWORK. Internet Archive: Wayback Machine [online]. [cit. 2020-05-25]. Dostupné z: https://web.archive.org/web/20120603140725/http://deepspace.jpl.nasa.gov/dsn/about.html

TWT Theory of Operation. Communications & Power Industries [online]. 811 Hansen Way Palo Alto, CA 94304-1031 [cit. 2020-05-25]. Dostupné z: https://www.cpii.com/docs/related/9/TWT%20THEORY%20COMPLETE.pdf

DAWSON, Stephen, Paul STELLA, William MCALPINE a Brian SMITH. Juno Photovoltaic Power at Jupiter. 4800 Oak Grove Drive, Pasadena, CA 91109.

JUNO SPACECRAFT: SOLAR ARRAYS. Mission Juno [online]. San Antonio, Texas, USA: Southwest Research Institute [cit. 2020-05-11]. Dostupné z: https://www.missionjuno.swri.edu/spacecraft/juno-spacecraft

DICKINSON, David. U.S. To Restart Plutonium Production for Deep Space Exploration. Https://www.universetoday.com/: universe today: space and astronomy news [online]. Fraser Cain, MARCH 20, 2013 [cit. 2020-05-11]. Dostupné z: https://www.universetoday.com/100875/u-s-to-restart-plutonium-production-for-deep-space-exploration/

KURTH, Bill. Juno Spacecraft Description. PDS: The Planetary Atmospheres Node [online]. Two Independence Square, Washington, D.C., United States: National Aeronautics and Space Administration, 2012, 2012-06-01 [cit. 2020-05-11]. Dostupné z: https://pds-atmospheres.nmsu.edu/data_and_services/atmospheres_data/JUNO/Juno%20Spacecraft%20Description.pdf

Juno Mission & Trajectory Design: Launch. Spaceflight101: Space News and Beyond [online]. [cit. 2020-05-31]. Dostupné z: https://spaceflight101.com/juno/juno-mission-trajectory-design/

In Depth: Juno. Solar System Exploration [online]. 4800 Oak Grove Dr, Pasadena, CA 91109, US: NASA [cit. 2020-06-08]. Dostupné z: https://solarsystem.nasa.gov/missions/juno/in-depth/

Planetary Protection. Office of Safety & Mission Assurance [online]. NASA [cit. 2020-06-08]. Dostupné z: https://sma.nasa.gov/sma-disciplines/planetary-protection

Juno Overview: Juno's Mythical Connection. NASA [online]. [cit. 2020-06-08]. Dostupné z: https://www.nasa.gov/mission_pages/juno/overview/index.html

WALL, Mike. Fastest-Ever Spacecraft to Arrive at Jupiter Tonight [online]. July 04, 2016 [cit. 2020-06-08]. Dostupné z: https://www.space.com/33336-nasa-juno-probe-jupiter-orbit-tonight.html

IESS, L., W. M. FOLKNER, D. DURANTE, et al. Nature. 2018, 555(7695). DOI: 10.1038/nature25776. ISSN 0028-0836. Dostupné také z: http://www.nature.com/articles/nature25776

KOWALKOWSKI, Theresa, Jennie JOHANNESEN, Try LAM a Try LAM. Launch Period Development for the Juno Mission to Jupiter. AIAA/AAS Astrodynamics Specialist Conference and Exhibit. Reston, Virigina: American Institute of Aeronautics and Astronautics, 2008, 2008-08-18, , -. DOI: 10.2514/6.2008-7369. ISBN 978-1-62410-001-7. Dostupné také z: http://arc.aiaa.org/doi/10.2514/6.2008-7369

Guillot, T., Miguel, Y., Militzer, B. et al. A suppression of differential rotation in Jupiter's deep interior. Nature 555, 227–230 (2018). https://doi.org/10.1038/nature25775

Kaspi, Y., Galanti, E., Hubbard, W. et al. Jupiter's atmospheric jet streams extend thousands of kilometres deep. Nature 555, 223–226 (2018). https://doi.org/10.1038/nature25793

Findings From NASA's Juno Update Jupiter Water Mystery. National Aeronautics and Space Administration [online]. [cit. 2020-06-10]. Dostupné z: https://www.nasa.gov/feature/jpl/findings-from-nasas-juno-update-jupiter-water-mystery

COULTER, Dauna, PHILLIPS, Tony, ed. A Freaky Fluid inside Jupiter? NASA Science [online]. August 9, 2011 [cit. 2020-06-10]. Dostupné z: https://science.nasa.gov/science-news/science-at-nasa/2011/09aug_juno3